Multimedia Tools and Applications manuscript No.
(will be inserted by the editor)

Visual Analytics for SpatioTemporal events

Ricardo Almeida Silva · João Moura Pires · Nuno Datia · Maribel Yasmina Santos · Bruno Martins · Fernando Birra

Received: date / Accepted: date

Abstract Crimes, forest fires, accidents, infectious diseases, human interactions with mobile devices (e.g., tweets) are being logged as spatiotemporal events. For each event, its geographic location, time and related attributes are known with high levels of detail (LoDs). The LoD plays a crucial role when analyzing data, enhancing the user's perception of phenomena. From one LoD to another, some patterns can be easily perceived or different patterns may be detected. Modeling phenomena at different LoDs is needed, as there is no exclusive LoD at which data can be analyzed.

Current practices work mainly on a single LoD, driven by the analysts' perception, ignoring that identifiyng the suitable LoDs is a key issue for pointing relevant patterns.

This paper presents a Visual Analytics approach called *VAST*, that allows users to simultaneously inspect a phenomenon at different LoDs, helping them to see in what LoDs patterns emerge or in what LoDs the perception of the phenomenon is different. In this way, the analysis of vast amounts of spatiotemporal events is assisted, guiding the user in this process.

The use of several synthetic and real datasets allowed the evaluation of *VAST*, which was able to suggest LoDs with different interesting spatiotemporal patterns and the type of expected patterns.

Acknowledgments This work has been supported by FCT - Fundao para a Cincia e Tecnologia MCTES, UID/CEC/04516/2013 (NOVA LINCS) and UID/CEC/00319/2013 (ALGORITMI), and COMPETE: POCI010145FEDER007043 (ALGORITMI).

Ricardo Almeida Silva and Nuno Datia*
ISEL and NOVA LINCS, Instituto Politcnico de Lisboa
*(*corresponding author*) E-mail: datia@isel.pt

João Moura Pires and Fernando Birra
NOVA LINCS, FCT, Universidade NOVA de Lisboa

Maribel Yasmina Santos
ALGORITMI Research Centre, University of Minho

Bruno Martins
INESC-ID and IST, University of Lisbon

Keywords Data Visualisation · Spatiotemporal Patterns · Multiple Levels of Detail · Visual Analytics

1 Introduction

A spatiotemporal event is a happening occurred in space and time. For example, *homicide((41.878037, -87.629442), 09/05/2015 20:00, 2)* represents a homicide that occurred at the latitude and longitude coordinates (41.878037, -87.629442), at eight o'clock PM of a given day, resulting in two victims. Spatiotemporal events can be described as data with the following structure: $event(S, T, A_1, \ldots, A_N)$, where S describes the geographic location of the event, T specifies the time moment, and A_1, ..., A_N are attributes detailing what has happened. Spatiotemporal patterns are non-uniform distributions of events across the space and time. Finding such spatiotemporal patterns helps to understand the associated phenomena Leipnik and Albert (2003); Ostfeld et al. (2005); Hering et al. (2009).

Nowadays, Visual Analytics (VA) approaches targeting the analysis of spatiotemporal events have been developed to analyse a single phenomenon (e.g., crimes), focusing on a specific kind of pattern (e.g, spatiotemporal hotspots) Maciejewski et al. (2010); Ferreira et al. (2013); Cho et al. (2016). However, patterns might appear in many different forms Shekhar et al. (2015). For example, in some phenomena, events form spatiotemporal clusters (e.g., tweets); in others, events form a cloud that moves in space throughout time (e.g., spreading of a disease); or, events occur spread out throughout space, but some regions reveal higher intensity (e.g., robberies). Therefore, focusing a specific type of pattern may leave many patterns undetected.

Also, most VA approaches have been designed to follow a single Level of Detail (LoD) analysis approach Zhang et al. (2012); Lins et al. (2013). Nevertheless, the LoD matters for the perception of patterns, and often there is no exclusive LoD to study phenomena Keim et al. (2008); Sips et al. (2012); Goodwin et al. (2016); Robinson et al. (2016). Although the LoD plays a crucial role in the perception of patterns, users have been left with the choice of the LoD to look for patterns.

In early stage of analysis, when users are not familiar with a spatiotemporal phenomenon, users often face difficulties to identify the LoDs in which patterns can be better perceived. They can easily fall into a condition of information overload Keim et al. (2008). By information overload, we mean, users likely face difficulties to identify the LoDs in which patterns can be better perceived.

To enhance analyses over spatiotemporal events, we propose to move from a single user-driven LoD to a multiple LoDs analysis approach, providing the user with an understandable high-level overview of the underlying structure of the phenomenon for each LoD. By understandable high-level overview, we mean several hints about the distribution of events in space or/and in time, which can provide a glimpse of the presence or absence of patterns. Following this approach, the user might detect very soon in what LoDs there are potential patterns, and of what kind they are.

A web-based VA tool anchored on the SUITE framework Silva et al. (2016), named *VAST* (**V**isual **A**nalytics for **S**patio**T**emporal events), is here proposed, designed, developed and evaluated. *VAST* allows users to simultaneously view hints about the absence or presence of different kinds of spatiotemporal patterns

at multiple LoDs. To the best of our knowledge, there is no other approach that simultaneously supports analyses over spatiotemporal events at multiple LoDs, completely independent from the application domain.

The evaluation of our proposal was conducted with two types of datasets of spatiotemporal events, namely (*i*) synthetic datasets and (*ii*) real datasets. Synthetic datasets with different spatiotemporal patterns at different LoDs were produced. For most cases, *VAST* could provide a correct overview of the phenomenon allowing us to identify the LoDs in which patterns exists and, therefore, the LoDs that should be used to detail the analysis. The real datasets studied were: (*i*) forest fires in Portugal; and (*ii*) violent attacks against civilians occurring in Africa; *VAST* was effective in identifying patterns present in these datasets, at different spatiotemporal LoDs.

The rest of the paper is organized as follows. The relevant related work is summarized at Section 2. Section 3 introduces the background information about granular theory for representing spatiotemporal data at different spatiotemporal LoDs. Section 4 details the interface of VAST, describing the way phenomena are analyzed at multiple LoDs. Section 5 presents the experiments carried out using synthetic and real datasets. Finally, we conclude and point out directions for future work in Section 6.

2 Related Work

Many approaches have been proposed in the literature that allow analyses over spatiotemporal events, in different research areas.

2.1 Information Visualization Approaches

To understand the dynamic of spatiotemporal events, animated maps (Andrienko and Andrienko (2006)) and change maps (Andrienko and Andrienko (2006)) are often used. However, maps only represent multi-attribute data and dynamism (Bédard et al. (2007); Aigner et al. (2011)); change maps are limited to small amounts of data and a few snapshots (each map representing a time instant or a time interval); the effectiveness of animated maps is therefore compromised (Tversky et al. (2002)).

The role of visualization is an open issue when dealing with numerous spatiotemporal events at high LoDs. The visualization methods get easily cluttered and become difficult to analyze (Silva et al. (2012); Li et al. (2016)). Visualization methods allowing the understanding of spatiotemporal events at different LoDs are still an issue that the information visualization's literature doesn't handle. This happens because a visualization needs to combine the spatial and temporal dimensions in a smart way in order be understandable, which, in our opinion and as you can see on the lines below, is quite challenging.

Aigner et al. (2011) make a comprehensive survey of techniques used for visualizing time-oriented data[1]. From the 115 visualization methods surveyed by (Aigner et al. (2011)), just 19 were designed to display spatiotemporal data. From

[1]The website: `www.timeviz.net`

these 19, 4 (Flow Map, Flowstrates, Space-time Path, Trajectory Wall) were designed to show movements of objects over time, which is out of the scope of this work.

From the remaining 15, 4 (GeoTime (Kapler and Wright (2005)), Space-time Cube (Kraak and Ormeling (2003)), Time Varying-Hierarchies on Maps (Hadlak et al. (2010)), Spatio-temporal event Visualization (Gatalsky et al. (2004))) make use of the space-time cube concept (X-Y to represent latitude and longitude and Z to represent time). In particular, Spatio-temporal event Visualization (Gatalsky et al. (2004)) was designed specifically for displaying spatiotemporal events so that they are placed within the space-time cube and the event's attributes can be encoded with visual variables like size, color, among others (Bertin et al. (1983)). However, 3D visualizations commonly suffer from occlusion and overplotting, making it difficult to grasp spatiotemporal patterns from their visual inspection.

A similar issue emerges from the 4 visualization methods (Data Vases (Thakur and Rhyne (2009)), Helix Icons (Tominski et al. (2005)), Pencil Icons (Tominski et al. (2005)), Wakame (Forlines and Wittenburg (2010))) that use 3D diagrams over geographic regions as well as from the 2 visualization methods (Icons on Map (Fuchs and Schumann (2004)), Value Flow Map (Andrienko and Andrienko (2004))) that use 2D diagrams to map the corresponding data values varying over time. Notice that, in order to use these last 6 mentioned visualization methods in a context of spatiotemporal events, we have to aggregate them by geographic regions. However, the diagrams can have a difficult readability if the number of geographic regions under study is high, or if they are quite close to each other.

The Time-oriented Polygons (Shanbhag et al. (2005)) might have also readability problems. This approach creates a partition of each polygon (2D) where each partition maps a value regarding a time period (using the color). The readability problems will emerge whether one considers small polygons or/and many time-periods. From the remaining results obtained, the most relevant for the analysis of spatiotemporal events might be: the Great Wall of Space-time (Tominski and Schulz (2012)), VIS-STAMP (Guo et al. (2006)) and Growth Ring Maps (Andrienko et al. (2011)).

VIS-STAMP (Guo et al. (2006)) is actually a visual analytics software package that couples computational, visual, and cartographic methods for exploring and understanding spatiotemporal and multivariate data. Although this approach allows the search for spatiotemporal patterns, this can only be done for one spatiotemporal LoD at a time.

The Great Wall of Space-time (Tominski and Schulz (2012)) creates a 3D wall based on a topological path over a cartographic representation. This wall is used to display how the data values associated to the geographic regions belonging to the path vary over time. This approach is not suitable to analyze spatiotemporal events because they are spread out in space and time. Therefore, we are not generally interested in a particular spatial path to analyze the phenomenon.

Growth Ring Maps (Andrienko et al. (2011)) is a technique for visualizing the spatiotemporal distribution of events. Every spatiotemporal event is represented by one pixel. Each location (for example the centroid of spatial clusters of events) is taken as the center point for the computation of growth rings. The pixels (i.e., events) are placed around this center point in an orbital manner resulting in the so called Growth Ring representations. The pixels are sorted by the time at which the event occurred: the earlier an event happened, the closer to the central

point the pixel is. Although this approach can be useful to provide a grasp on the spatiotemporal distribution of events, a clear understanding about when spatiotemporal hotspots occurred can be hard to achieve through visual inspection, for example. Furthermore, there might be others patterns that are not captured like changes in the structure of the spatial distribution of events throughout time.

As mentioned, the design of a visualization method that aims to combine the spatial and temporal dimension of data is not trivial. Perhaps that's why from 115 visualization methods surveyed by (Aigner et al. (2011)), we only have 19 visualization methods for spatiotemporal data. Their usage for spatiotemporal events was further discussed in this work, and in short, they have some problems handling spatiotemporal events. Another characteristic which is transversal to the visualization methods discussed is that they encode data into visual representations at certain LoDs. In fact, from our perspective, the visualizations should be used according to the LoD of the input data in spite of the issues identified for using them. For instance, Spatiotemporal event Visualization (Gatalsky et al. (2004)) should be used when spatiotemporal events are provided at high LoDs (latitude and longitude coordinates) while the Time-oriented Polygons (Shanbhag et al. (2005)) should be used when the events are aggregated by some administrative level (e.g., counties) and by year.

In general, a visualization method produces a single representation of data. In order to make this representation effective, the visualization methods are designed taking into account the analytical goal and sometimes the data (Aigner et al. (2011)). However, the analysis of spatiotemporal data frequently requires coordinated views in order to deal with the spatial, temporal, and thematic aspects of data simultaneously (Dykes et al. (2005)). This approach has become standard in the recent applications of visual analysis because they directly support the expression of complex queries using simple interactions (Scherr (2008); Dykes et al. (2005); Weaver (2010)).

2.2 Automated Approaches

Shekhar et al. (2015) provide a survey about spatiotemporal pattern families. The main families identified are spatiotemporal outliers, spatiotemporal coupling, spatiotemporal partitioning or summarization, and spatiotemporal hotspots.

A spatiotemporal outlier is a spatially and temporally referenced object or event whose non-spatiotemporal attribute values differ significantly from those of other objects in its spatiotemporal neighborhood. For example, spatiotemporal outlier detection can be used to detect the occurrence of unexpected events like crimes or traffic accidents. Spatiotemporal coupling patterns represent spatiotemporal objects or events which occur in close geographic and temporal proximity. For example, analysis of crime datasets may reveal frequent occurrence of misbehaviors and drunk driving after and near bar closings on weekends. Spatiotemporal clustering is the process of grouping similar spatiotemporal objects or events, and thus partitioning the underlying space and time. For example, partitioning and summarizing crime data, which is spatial and temporal in nature, helps law enforcement agencies find trends of crimes and effectively deploy their police resources (Chen et al. (2004); Malik et al. (2010)). Spatiotemporal hotspots are regions jointly with certain time intervals where the number of objects or events is

anomalously or unexpectedly high. For example, in epidemiology finding disease hotspots allows officials to detect an epidemic and allocate resources to limit its spread (Gabriel et al. (2013)).

Several algorithms have been developed to compute spatial and spatiotemporal patterns and a survey on them can be found in (Roddick and Spiliopoulou (1999); Miller and Han (2009); Shekhar et al. (2015)).

Often, the patterns have statistical expression. This way, spatial or spatiotemporal statistics are proposing quantitative analysis about the presence or absence of such patterns. The average nearest neighbor index (Ebdon (1985)) (ANN) can give some hints about the presence of spatial clustering. If ANNs value is less than one, the pattern exhibits clustering. Otherwise the trend is toward dispersion. Getis-Ord General G (Getis (1992)) measures how concentrated the high or low values are for a given study area. Positive scores indicate that the spatial distribution of high values is spatially clustered and the negative scores indicate that the spatial distribution of low values is spatially clustered. Getis-Ord General G measure might also suggest spatial outliers (Getis (1992)). Global Moran's I (Moran (1950)) measures the spatial autocorrelation or dependency based on feature locations and an associated attribute. When the spatial distribution of high values and/or low values in the phenomena is more spatially clustered than would be expected if underlying spatial processes were random, the Global Moran's I value will be positive. The spatiotemporal statistics methods like Knox (Knox and Bartlett (1964)), Mantel (Mantel (1967)) and the Jacquez k-nearest neighbor test (Jacquez (1996)), measures the level of spatiotemporal interaction embedded in a phenomenon. More recently, Gabriel et al. (2013) proposed estimators to measure the spatiotemporal clustering/regularity in spatiotemporal point processes (equivalent terminology for spatiotemporal events with point as their spatial representation).

One challenge to mine spatiotemporal data results from the Modifiable Area Unit Problem (MAUP) (Openshaw (1984)) or multi-scale (i.e., multiple LoD) effect, since the results depend on a choice of appropriate spatial and temporal scales (i.e., LoDs) (Swedberg and Peuquet (2016)). This means that patterns may be biased due to how data is aggregated/summarized. Analyses across multiple LoDs can make the MAUP identifiable or discarded sooner. For example, when a pattern is only visible in a specific LoD it can be further validated. One might conclude that the pattern suffers from MAUP and can be ignored or, if the phenomenon specifically operates there, it can be considered valid. Therefore, we argue that the analysis across multiple LoDs can attenuate the MAUP.

2.3 Visual Analytics Applications

There are several applications/prototypes to make analyses over spatio-temporal events. In the project carried out by Lahouari et al. Lahouari et al. (2014), 47 applications/geovisualization methods were assessed. Among the applications studied, 25% (12) were developed to analyze phenomena logged as spatiotemporal events. None of the approaches support data view at multiple spatial and temporal granularities (i.e., st-LoDs).

VA approaches also have been proposed in the literature. Some of these preview VA approaches support separate analyses of space and time anchored on descriptive statistics, most commonly considering one st-LoD at a time.

Lins et al. (2013) propose a compressed hierarchical data structure to hold huge amounts of spatiotemporal events in memory. In addition, the authors implemented some web-based applications to explore real datasets of spatiotemporal events. The spatial LoD at which the events are displayed changes according to the zoom level. However, the same behavior was not registered when the time series was analyzed. Besides that, the interface contains a line chart with the number of events aggregated by day. This approach does not focus on a particular analytical goal but these are addressed using the descriptive statistic $\mathbb{COUNT}$. Another characteristic is the fact that this approach is independent from the phenomenon. Furthermore, and although they have spatiotemporal events available at different spatial and temporal LoDs, their analyses are conducted using one spatial or temporal LoD at a time, separately.

Ferreira et al. (2013) develop a visual environment to explore taxi trips, called *TaxiVis*. Analyzing it, the input data are events of taxi pickups and taxi drop-offs that happened in New York City. This approach supports exploratory analysis about taxi pickups and taxi drop-offs without any particular analytical task in mind. They are addressed using descriptive statistics that result from the separate analysis of the spatial and the temporal dimension of data.

Some of the VA approaches discussed support separate analyses of space and time and these analyses are performed at one spatiotemporal LoD at a time like the works (Lins et al. (2013); Ferreira et al. (2013); Cho et al. (2016)) discussed in detail here. More similar approaches were found (Kisilevich et al. (2010); Malik et al. (2010); MacEachren et al. (2011); Andrienko et al. (2013); Cho et al. (2016)).

Others approaches support analyses that look for spatiotemporal patterns like Guo et al. (2006) or Maciejewski et al. (2010). However, these kinds of approaches follow analyses based on a single LoD, and in some cases, they are developed for the detection and exploration of a particular spatiotemporal pattern in a particular domain application (Wang et al. (2013); Chae et al. (2012); Thom et al. (2012)).

As opposed to that, we aim to give an overview of the presence of absence of spatiotemporal patterns at different LoDs simultaneously without focusing in a particular application domain but just considering phenomena logged as spatiotemporal events.

2.4 Manifold LoDs Approaches

The scale (or LoD) of analysis can greatly affect results (e.g., MAUP). This issue has been acknowledged a long time ago (Openshaw (1984)). However, with spatiotemporal events in mind, analytical approaches have been mainly developed to support analyses based on a single LoD. Thus, the MAUP becomes a problem, once unsuitable LoDs can hide patterns and conceal the true underlying nature of a dataset.

VA approaches working across LoDs are still in its infancy despite the fact that they have been gaining more attention in recent years. Sips et al. (2012) propose a Visual Analytics approach called *Pinus*, aiming at the detection of patterns at multiple temporal LoDs in numerical time series, specifically from environmental

sciences. To accomplish that, statistical measures are computed for all possible time LoDs (i.e., scales) and starting positions, namely, mean, variance, and discrete entropy were implemented. This approach makes no assumption about the temporal LoD and the temporal patterns. It combines statistic measures and the pattern recognition abilities of the user to support effective detection of temporal patterns at different temporal LoDs. We aim to bring this mindset for the analysis of spatiotemporal events at several spatiotemporal LoDs.

Goodwin et al. (2016) propose a framework for analyzing multiple variables across spatial LoDs and geographical locations. Based on it, they developed a suite of novel interactive visualization methods to identify interdependencies in multivariate data coupled with a series of correlation matrix views. This approach does not focus on a particular phenomenon and was devised to look for correlations on multiple variables in multiple spatial LoDs and geographic regions.

Robinson et al. (2016) developed a visual analytics approach, called STempo, to support the discovery of patterns found in spatiotemporal events. STempo was designed to detect and analyze significant co-occurrences of real-world events. This approach is making a separate analysis of the temporal and spatial dimension of events as the input for the T-pattern algorithm corresponds to records containing the timestamp and a set of event types that occurred in it. Finally, this approach looks for temporal patterns and not for spatiotemporal patterns, because the sequences identified are not assigned to specific geographic regions, for instance. Nevertheless, this approach computes temporal patterns in multiple temporal LoDs.

The visual analytics approaches discussed so far explore time following a linear model. However, periodicity is underlying in all societies. Swedberg and Peuquet (2016) propose a visual analytics web application developed to help users in the detection and analysis of calendar related periodicity in spatiotemporal event data sets via exploratory user interaction. This work allows for the analysis at multiple spatial LoDs and temporal LoDs despite the fact that the number of the spatial LoDs that we can analyze, simultaneously, are limited to two (raw data and aggregated by the user-defined geographic regions). Although the mentioned patterns are interesting, they are obtained by working with space and time separately using only the descriptive statistic $\mathbb{COUNT}$.

To the best of our knowledge, there are no approaches that work across several spatial and temporal LoDs, working with space and time together, and therefore, looking for spatiotemporal patterns at different spatiotemporal LoDs. Furthermore, the VA approaches discussed do not have any theoretical foundation that anchors the analysis across LoDs. The approaches rely on clever visual designs that show data at different LoDs. However, from our perspective, a theoretical foundation that anchors the analysis across LoDs can be important for having phenomena representations for different LoDs, and then, use better suited visualization methods to display them.

3 Primer on Granular Theory

Granular computing has emerged as a paradigm of knowledge representation Yao et al. (2013), where granules are basic ingredients of information. Roughly, a granularity defines a division of a domain in a set of granules disjoint from each other

Silva et al. (2015a). *Counties* and *States* are common examples of spatial granularities; *Hours* and *Days* are examples of temporal granularities.

Under a general theory of granularities Silva et al. (2015a), a granular computing approach was devised to model spatiotemporal phenomena at multiple LoDs. This approach was labeled as the granularities-based model Silva et al. (2015b), where a phenomenon is modeled through a collection of statements. Granules are used in the statements' arguments. For example, we can model a crime event through the statement: *crime*(*Oakland*, 03/01/2015 18*h*, 1, *homicide*) where the granules used come from the granularities *Counties*, *Hours*, *Natural Numbers*, and *Crime Types*.

Statements are made at some LoD. The set of granularities involved in the statement defines the LoD at which an event is described. For example, the LoD of *crime*(*Oakland*, 03/01/2015 18*h*, 1, *homicide*) is defined by the corresponding granularities: *Counties*, *Hours*, *Natural Numbers*, and *Crime Types*. Through the granularities-based model, statements can be generalized to coarser LoDs automatically. Using the granularities-based model, we are able to have a phenomenon modeled in multiple LoDs Silva et al. (2015b).

Let us consider a statement describing an event using a spatial granule $s \in S$ and temporal granule $t \in T$. The pair (s, t) is called a spatiotemporal granule (st-granule) of the spatiotemporal LoD (S, T).

Each st-granule (s, t) indexes the set of statements spatially located at s and temporally located at t. Typically, at a very detailed spatiotemporal LoD (from this point forward referred as st-LoD), events are sparse and mostly non-co-occurring. This means that either st-granules have no events, or have just one event. At coarser st-LoDs, the co-occurrence of events on the same st-granule becomes more likely.

On top of the granularities-based model, Silva et al. Silva et al. (2016) developed a SUmmarizIng spatioTemporal Events framework (SUITE) that builds, for each st-LoD, summaries about phenomena represented as spatiotemporal events, called *abstracts*. Abstract values can be a number, a vector, or a matrix. SUITE consider five types of abstracts: *(i)* Global; *(ii)* Spatial; *(iii)* Temporal; *(iv)* Compact Temporal; and *(v)* Compact Spatial.

A Global Abstract summarizes all statements by a single abstract value. Known spatiotemporal statistics Shekhar et al. (2015); Gabriel et al. (2013) (e.g., the Knox or Mantel statistics) can be used to compute Global Abstracts. A Spatial Abstract summarizes, for each $t \in T$, all statements at t by a single abstract value, so we get a time series of abstract values, each one summarizing the spatial distribution of the events at granule t. Known spatial statistics Ebdon (1985); Shekhar et al. (2015) (e.g., Average Nearest Neighbor or Moran's I) can be used to compute spatial abstracts.

A Temporal Abstract summarizes, for each $s \in S$, all statements at s, by a single abstract value, so we get a map of abstract values, each one summarizing the temporal distribution of the events at granule s. Known temporal statistics Box et al. (2015) can be used to compute temporal abstracts.

A Compact Temporal Abstract is just a summarization of a Temporal Abstract, i.e., a summarization of a time series of abstract values into a single abstract value. Similarly, a Compact Spatial Abstract is just a summarization of a Spatial Abstract, i.e., a summarization of a map of abstract values into a single

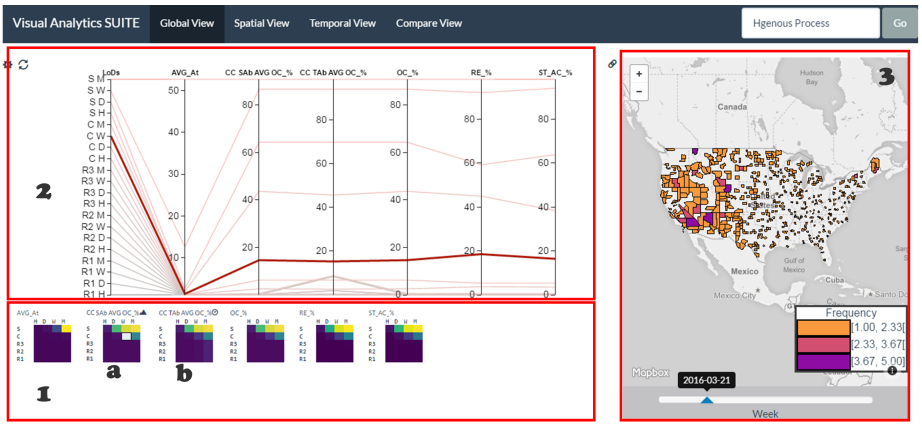

Fig. 1 An overview of the *VAST* interface.

abstract value. ST-Abstracts will refer either the Global Abstracts or the Compact Temporal Abstracts or the Compact Spatial Abstracts.

4 Visual Analytics for SpatioTemporal events

Visual **A**nalytics for **S**patio**T**emporal events (*VAST*)[2] was developed to support analyst in the task of visually inspecting the computed abstracts at many LoDs simultaneously, allowing users to understand not only the absence or presence of different kinds of spatiotemporal patterns, but also at which LoDs they are visible or at least in what LoDs they are more easy to be found. *VAST* implements the granularities-based model and the SUITE framework, including the abstracts presented in Appendix A.

VAST's design follows the VA Mantra: *"Analyze first, show the important, zoom, filter and analyze further, details on demand*" Keim et al. (2008). First of all, the interface starts by displaying ST-Abstracts at all available st-LoDs. This interactive visualization may provide hints about different patterns within the spatiotemporal events. Then, one can analyze further by looking at Spatial Abstracts (time series of abstract values) or Temporal Abstracts (i.e., "maps" of abstract values). At any moment of the analysis, it is possible to visually inspect the actual spatial distribution of the phenomenon at a specific temporal granule t in a particular st-LoD.

The interface is composed of three main areas, as illustrated in Fig. 1:

1. **ST-Abstracts**;
2. **Dynamic Abstract Area**;
3. **Phenomena Representation**.

The first area, **ST-Abstracts** (Fig. 1-1), displays a matrix plot for each ST-Abstract. The symbol ▲ points out a Compact Spatial Abstract (e.g., Fig. 1-1.a) while the symbol ⏲ indicates a Compact Temporal Abstract (e.g., Fig. 1-1.b).

[2]VAST prototype can be tested online at `http://staresearch.net/resource#prototypes`.

When none of these icons is present we have a Global Abstract. Each cell of a matrix plot shows the value of an ST-Abstract at a st-LoD. The skeleton of a matrix plot is displayed in Fig. 2. In the rows, we have the spatial granularities (finer granularities at bottom), and in the columns we have the temporal granularities (finer granularities at left). All used abstract values are numbers and their value is mapped to a color using the color scheme shown in Fig. 2. For example, Fig. 1-1 shows 6 matrices, from left to right:

- a Global Abstract named *Average Atoms in st-granules*;
- a Compact Spatial Abstract named *Average of Spatial Occupation Rate*;
- a Compact Temporal Abstract named *Average of Temporal Occupation Rate*;
- three more Global Abstracts respectively *Occupation rate*, *Reduction rate* and *Collision Rate*.

All matrices are using 5 spatial granularities (State, County, and 3 rasters) and 4 temporal granularities (hours, days, weeks, and months).

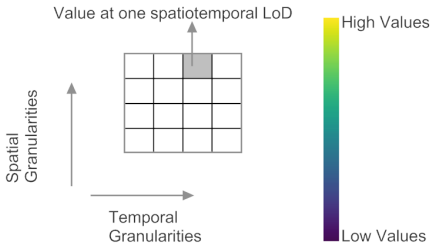

Fig. 2 An overview of the structure of a matrix plot.

The **Dynamic Abstract Area** (Fig. 1-2) is used to present 3 different visualizations: (*i*) a **Global View** that shows a Parallel Coordinates visualization with

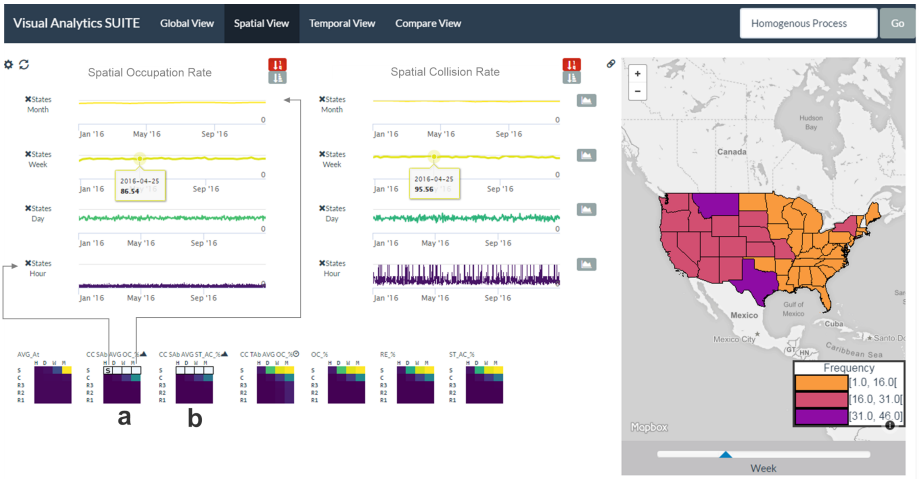

Fig. 3 An overview of the *VAST* interface with Spatial Abstracts.

the same abstracts presented in the ST-Abstracts area; (*ii*) a **Spatial View** that shows the time series corresponding to a few selected Spatial Abstracts, as illustrated in Fig. 3; and, (*iii*) a **Temporal View** that shows the maps corresponding to a few selected Temporal Abstracts, as illustrated in Fig. 4.

In the Parallel Coordinates visualization (Fig. 1-2) each line corresponds to one st-LoD. The most left coordinate represents the st-LoDs ordered from the more detailed st-LoD (*R1*, *Hour*) to the coarser st-LoD (*State*, *Month*). The other coordinates correspond to the ST-Abstracts presented in ST-Abstract area.

In Fig. 3, there are four cells selected from *Average of Spatial Occupation Rate* (Fig. 3.a) and from *Average of Spatial Collision Rate* (Fig. 3.b). Therefore, eight Spatial Abstracts are visible in the Spatial View, which are organized/grouped by Spatial Abstract and ordered from the more detailed st-LoD to the coarser one.

The Temporal View is illustrated in Fig. 4 and there are two st-LoDs selected from the *Average of Temporal Occupation Rate* (see Fig. 4.b): (*R3*, *Weeks*) and (*Counties*, *Days*). As a result, two Temporal Abstracts are displayed. When the st-LoD has a *raster* granularity, the map represents each spatial granule through a point, leading to a dot map (e.g., the map on the right side). Otherwise, the spatial granules are displayed in their original form, which leads to a choropleth map (e.g., the map on the left side).

The last area is the **Phenomena Representation** (Fig. 1-3) used to display spatiotemporal events at a st-LoD using thematic maps. The slider underneath allows the user to scroll temporally through the temporal granules, according to the st-LoD that was chosen. The map displays the number of events for each st-granule.

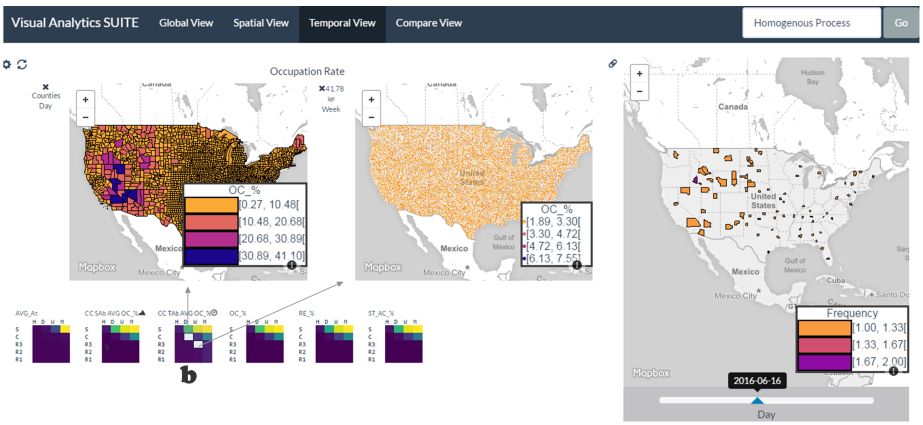

Fig. 4 An overview of the *VAST* interface with Temporal Abstracts.

4.1 Main Abstracts Implemented

Several abstracts were implemented and actually proposed in the context of this work. Whenever some abstract are based on another work a reference will be placed. A subset of abstracts implemented/proposed are described:

1. The **Occupation rate** measures the percentage of spatiotemporal granules occupied, that is, measures the average density of a model at a given LoD. The value 0 means no spatiotemporal granules are occupied and 100 means that all spatiotemporal granules are occupied.
2. The **Collision rate** measures the percentage of the spatiotemporal granules occupied that index more than one event, that is, it measures the average co-occurrence of a model at a given LoD. In this case, 0 means no co-occurrence of events in spatiotemporal granules and 100 means that any spatiotemporal granule has events co-occurring.
3. The **Granular Mantel Bounded and Normalized (GMBN)** measures the spatiotemporal interaction among granular syntheses. The purpose of this measure is to have a hint of the presence or absence of spatiotemporal clustering pattern or any other pattern that involves spatiotemporal interaction like the contagious process. The value ranges between 0 and 1 where 0 means no interaction at all among the granular syntheses and 1 means that all the spatiotemporal granules are interacting among each others. The GMBN receives as input parameters the spatial and temporal distances. These distances are expressed in terms of granular extents with respect to the spatiotemporal LoD in which the GMBN is computed.

Spatial Abstracts hold a summary for each temporal granule about the granular syntheses occurred on it. The Spatial Abstracts considered are:

1. The **Spatial occupation rate** is computed in the scope of each temporal granule. The values interpretation is similar to the one presented considering the global abstract. This way, we can track the temporal evolution of the occupation rate.
2. The **Spatial frequency rate** measures for each temporal granule the percentage of atoms occurred on it given all the atoms of the phenomenon at a given LoD. In other words, corresponds to a frequency distribution normalized by the total number of atoms in the phenomenon at particular LoD. The range of values for this abstract lies between 0 and 1 (in each temporal granule) so that 0 means that no atom occurred on that temporal granule while 1 means all the atoms occurred on that temporal granule. Through this abstract, we aim to understand how the intensity of the phenomenon spreads out throughout time. This is abstract is not a novel contribution.
3. The **Spatial average nearest neighbor (Spatial ANN)** measures how occupied spatiotemporal granules are dispersed or clustered in each temporal granule. This might indicate variations between dispersed and clustered spatial distributions. The value computed is not a distance but a normalized value such that if the value is less than 1, the spatial pattern might be clustering while if the value is greater than 1, the trend is toward dispersion. Notice that, the z-score[3] of the Spatial ANN is also computed. Very low or very high z-score

[3] `http://mathworld.wolfram.com/z-Score.html`

values suggest some spatial pattern, and therefore, we can reject the complete spatial randomness. This abstract was developed based on Ebdon (1985).
4. The **Spatial scope** measures the percentage of spatial area occupied by the phenomenon in each temporal granule, where the spatial area is a concave region that encloses all the granular syntheses, and the total spatial area corresponds to the extent of the spatial granularity. Through this abstract, we aim to understand if the spatial scope of the phenomenon varies throughout time.
5. The next Spatial Abstract, considers two consecutive temporal granules t_{i-1}, t_i. For each one, a region that encloses all spatiotemporal granules is computed. Then, the centroids of each region are computed, and the value of the Spatial Abstract at t_i consists of the distance between the centroid at t_{i-1} and the centroid at t_i. This is done for all temporal granules apart from t_0 where the Spatial Abstract takes the value 0. We call this Spatial Abstract as the **Spatial Consecutive Distance Between Centers of Mass**. Through this abstract, we aim to understand whether the phenomenon moves in space throughout time.

Temporal Abstracts hold a summary for each spatial granule about the granular syntheses occurred considering all temporal scope. The Temporal Abstracts considered are:

1. The **Temporal occupation rate** is, in this case, computed in the scope of each spatial granule. The values' interpretation is similar to the one presented considering the Occupation rate. This way, we can assess the occupation rate over the space.
2. The **Temporal frequency rate** measures for each spatial granule the percentage of atoms occurred on it given all events of the phenomenon at a given LoD. The range of values for this abstract lies between 0 and 1 (in each spatial granule) so that 0 means that no event occurred on that spatial granule while 1 means all the events occurred on that spatial granule. This way, we can observe the intensity of the phenomenon over the space.
3. A Temporal Abstract **Temporal average nearest neighbor** measures how occupied spatiotemporal granules are dispersed or clustered in time for each spatial granule. The interpretation of values is similar to the one presented in the case of the Spatial average nearest neighbor. Furthermore, the corresponding z-score was also implemented.

5 Experiments

VAST was used to conduct experiments over two types of datasets of spatiotemporal events: (*i*) seven synthetic datasets; (*ii*) two real datasets.

5.1 Synthetic Datasets

The synthetic datasets of spatiotemporal events were generated using the stpp R package (Gabriel et al. (2013)). Sttp exposes a set of functions to simulate spatiotemporal events following different models (Gabriel et al. (2013); Gabriel (2014); Møller and Ghorbani (2010)):

1. **Homogeneous Poisson Process**: the homogeneous Poisson process is the simplest mechanism for the simulation of a spatiotemporal point pattern. This model hardly approaches a pattern in a phenomenon but provides a good basis for comparison as it reflects complete spatiotemporal randomness. Informally, in a homogeneous Poisson process, the events form an independent random sample from the uniform distribution on the spatiotemporal domain in which the events were simulated.
2. **Poisson Cluster Process**: the Poisson cluster process simulates spatiotemporal clusters of events. This model might reflect phenomena such as forest fires where several wildfire occurrences appear close in time and space, or the presence of spatiotemporal hotspots of crimes, for instance. Informally, a set of parents are generated, and afterward, a set of events are generated around each simulated parent. The dispersion of events in space and in time around each parent event is an input parameter through which we specify the st-LoD. In this process, when events happen they occur near to each other in space and time. However, it is possible that no events occur.
3. **Contagious Process**: A contagious process can be pictured out as a cloud of events moving in space throughout time. The contagion process of a disease, for example, in which the disease is transmitted to other people through direct contact with an infected person. Informally, an initial event is generated, and afterward, the next events are generated near to locations of the previous event(s) simulated. The spatial and temporal neighborhoods on which the next events are generated are input parameters through which we specify the st-LoD.
4. **Log-Gaussian Cox Process**: The Log-Gaussian Cox process simulates spatiotemporal events such that some regions reveal higher intensity. This model might reflect phenomena that contain geographic regions of higher risk, which might changes slowly over time. This pattern might happen with wildfires, infectious diseases, among others. Informally, the Log-Gaussian Cox process is a in-homogeneous Poisson process with a stochastic (i.e., randomly determined) intensity. In this case, we have no precise control of the st-LoD in which the pattern is simulated.

Different datasets were produced following one or more of the models presented. The set of datasets simulated are displayed in Table 1 along with their characteristics like the model used to generate it, the number of events, and the spatiotemporal LoD in which the pattern/model was simulated.All the datasets were generated within the region of the USA and during one year.

Table 1 Datasets of spatiotemporal events simulated.

	Model	Number Events	LoD
Dataset 1	Homogenous	30.000	NA
Dataset 2	Poisson Cluster	30.000	110 Km, Day
Dataset 3	Poisson Cluster	30.000	2 Km, Week
Dataset 4	Poisson Cluster + Homogenous	33.000	110 Km, Day
Dataset 5	Poisson Cluster	30.000	570 Km, Week
Dataset 6	Contagious	5.000	110 Km, Week
Dataset 7	Log-Gaussian Cox	15.000	NA

5.1.1 Poisson Cluster Process

Let's start by the Dataset 2. This dataset was simulated with the Poisson Cluster process and is composed by 30.000 events within the region of the USA that occurred during one year. The clusters of events are built around a parent within a spatial distance of 110 km and a temporal distance of one day.

Regarding Dataset 2, the most detailed spatial granularity *Raster* $(0.16km^2)$ is based on grid of 16384 x 16384 cells that cover the analyzed spatial extent of the phenomenon, and each cell has an area of 0.16 km^2. The coarser spatial granularities were obtained by dividing by a factor of 4 the number of cells in the grid. So the valid granularities for space were rasters with cell sizes approximately of 0.16 km^2 (R1), 2.55 km^2 (R2), and 40.74 km^2 (R3). The granularities *Counties* and *States* were also included. The time granularities used were *Hours*, *Days*, *Weeks*, *Months*.

The raw data (events) were encoded at at the finer st-LoD, which includes the time granularity *Hours* and the space granularity R1. After that, the granularities-based module was used to automatically produce the data for all LoDs and the *VAST* was used to precompute all the abstracts defined for each LoD.

We started by looking at global abstracts. Fig.5 shows the global abstracts (i.e., the *Occupation rate*, the *Collision rate* and the GMBN) for all the st-LoDs of Dataset 2.

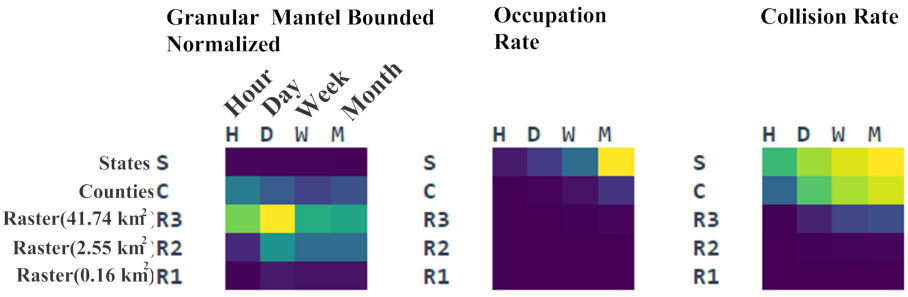

Fig. 5 Global Abstracts: *GMBN*, *Occupation rate* and *Collision rate* describing Dataset 2.

The *GMBN* points to the st-LoD - (R3, *Days*) as the one with greatest spatiotemporal interaction. This seems to be compliant with the st-LoD in which the pattern was simulated. Regarding the other global abstracts (i.e., the *Occupation rate*, and the *Collision rate*), their values increases as long as we move to coarser st-LoD. This happens because as long as we move to coarser st-LoD, the co-occurrence of granular syntheses in spatiotemporal granules increase, once the number of spatiotemporal granules available at coarser st-LoD decreases. Nevertheless, according to the phenomenon, the values of *Occupation rate* and *Collision rate* might increase at different rates.

To better understand in what st-LoD the perception of the phenomenon distinguishes itself, we use an instrument from the interface module that allows us to correlate two global abstracts.

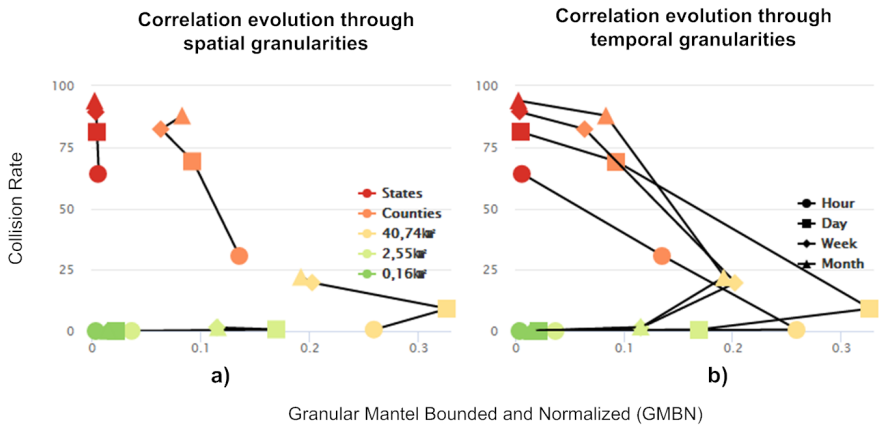

Fig. 6 Correlation between the GMBN and the Collision rate.

We have implemented two forms of observing the correlation between two global abstracts. One of them is named correlation evolution through spatial granularities, which allows to observe for each spatial granularity how the correlation behaves, considering all the temporal granularities. The other is named correlation evolution through temporal granularities, which allows us to observe for each temporal granularity how the correlation behaves with respect to all the spatial granularities.

Fig.6a illustrates the correlation evolution through spatial granularities between the GMBN and the Collision rate. Each spatial granularity corresponds to a line in the chart. On the other hand, Fig. 6b illustrates the correlation evolution through temporal granularities between the GMBN and the Collision rate. In this case, each temporal granularity corresponds to a set in the chart. The color encodes the spatial granularity while the shape of the markers encodes the temporal granularity. This encoding scheme is the same on both forms of correlation. Therefore, a marker with a particular color and shape represents the same spatiotemporal LoD on both charts.

Moreover, in the correlation evolution through spatial granularities the lines connect markers with the same color (i.e., the spatial granularity is the same) while in the correlation evolution through temporal granularities the lines connect markers with the same shape (i.e., the temporal granularity is the same). Notice that both charts might become cluttered according to the data that are being mapped. To attenuate that problem, a user can hide or make visible series of the chart interacting with the legend.

On both charts we can observe “elbows”. An “elbow” tip, in these charts, has a particularity that it might be interesting to explore. For the discussion that follows, lets assume that an elbow is created by going from a finer granularity to a coarser granularity (e.g., as happens in the series regarding the spatial granularity $40,74km^2$ (R3) in Fig.6a. In these cases, it seems that there is a granularity G such that: (i) for granularities finer than G the correlation seems to be positive; (ii) for granularities coarser than G the correlation seems to be negative. This might

be a hint about the LoDs in which the perception of a phenomenon distinguishes itself, considering the two global abstracts at study.

In Fig.6a, an "elbow" is visible taking into account the spatial granularity R3, where the elbow tip is reached at the granularity *Days*. In Fig.6b, the "elbow" most pronounced is revealed at the temporal granularity *Days* where the "elbow" tip is reached at the granularity R3.

Therefore, the st-LoD - (R3, Days) is where the "elbow" tip is observed on both charts. This conclusion is similar to the one achieved by just looking at the GMBN, in Fig.5, and this analysis might seem useless. However, looking at only one Global Abstract as a way of understanding suitable st-LoDs to detail our analyses might be misleading. These scenarios will be discussed later.

The correlation between the GMBN and the Collision rate serves two purposes. First, there is one more hint pointing to (R3, Day) as a suitable st-LoD to analyze the data. Second, it allows us to introduce the correlation charts.

Given the evidences pointing that there might be a pattern in the st-LoD - $(R3, Days)$, or at least the phenomenon is observable in such st-LoD, we use the *Phenomenon Representation* area to have a grasp of the data at such st-LoD. The data at three different temporal granules chosen without any particular criterion are displayed in Fig.7. As you can see, there are clusters of events happening over the USA.

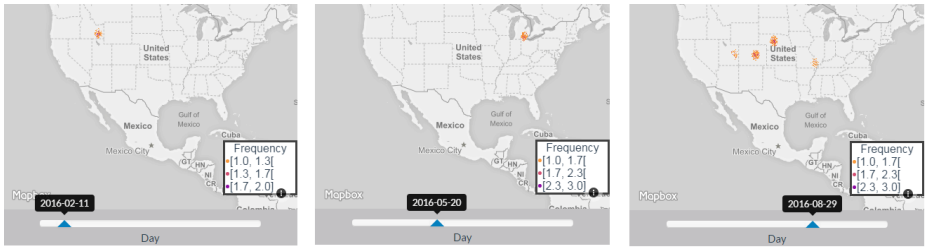

Fig. 7 Dataset 2 at the spatiotemporal LoD R3 and *Days* displayed in three temporal granules.

The analysis made so far points out that the Dataset 2 (see Table 1) might have a spatiotemporal pattern and such pattern might be better perceived at R3. The pattern in question are clusters of events happening over time. Our analyses were further detailed using the Spatial and the Temporal Abstracts to confirm a pattern in the st-LoD - $(R3, Days)$.

We start by looking to the Temporal Abstract - Temporal Center Masss Positioning for three st-LoD as can be seen in Fig.8. The st-LoD are: $(R3, Days)$, $(Counties, Days)$ and $(States, Days)$. Orange means that most of the events that occurred in the spatial granule were old while dark blue means that most of the events occurred in the spatial granule were recent in what concerns the extent of the temporal granularity.

Looking at the st-LoD - $(R3, Days)$ and $(Counties, Days)$, in Fig.8, the geographic regions where the clusters of events have happened can be identified, since spatial granules close to each other have similar values of the Temporal center masss positioning. In other words, the events occurring near in space seems to occur near in time.

The previous conclusions are also captured by the two Compact Temporal Abstracts of the Temporal center mass's positioning, i.e., its Coefficient of Variation and its Spatial autocorrelation. In this case, the coefficient of variation tells us in what st-LoD the value of the Temporal Center Mass's Positioning varies more among the spatial granules while the Spatial autocorrelation measures how the value of the Temporal Center Mass's Positioning is similar in neighboring spatial granules. Thus, we are interested in st-LoD such that there is a considerable variation and the spatial autocorrelation's value suggests spatial correlation. In what concerns the three st-LoD displayed in Fig.8, the st-LoD - $(R3, Days)$ is where the Coefficient of Variation and the Spatial autocorrelation take the highest values as detailed in Fig.8. The spatial autocorrelation is 0.94 (strong positive correlation) and the coefficient of variation is 0.64. Clusters are spread out across the entire USA. Besides that, we can relate the geographic regions and the time moments in which the clusters occurred. This kind of perception is lost if you look at the data in the st-LoD - $(States, Days)$ (see Fig.8), for example.

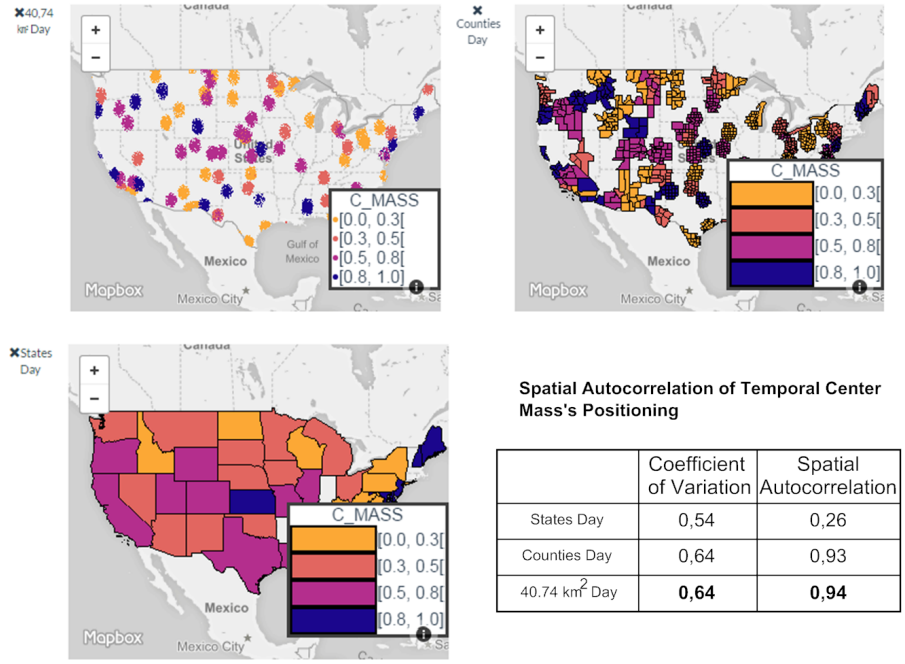

Spatial Autocorrelation of Temporal Center Mass's Positioning

	Coefficient of Variation	Spatial Autocorrelation
States Day	0,54	0,26
Counties Day	0,64	0,93
40.74 km^2 Day	**0,64**	**0,94**

Fig. 8 The Temporal Center Mass's Positioning for three st-LoD.

Since clusters are happening over time, we use the Compact Spatial Abstract - Spatial average nearest neighbor (Spatial ANN) and its z-score to understand when those clusters of events are happening.

Four st-LoD were chosen: $(R3, Hours)$, $(R3, Days)$, $(R3, Week)$, $(R3, Month)$. These were chosen because, based on evidence, we know that st-LoD - $(R3, Days)$ is appropriate to analyze the data. So, the st-LoD - $(R3, Days)$ is included in the next analysis. This leaves us with the possibility of varying the spatial or the

temporal granularity. But the previous analysis allows to note that the spatial granularity $R3$ was able to show the places where the clusters happened. For this reason, we vary the temporal granularity.

The Spatial Abstracts are displayed in Fig.9. Notice that, the set of time series for each Temporal Abstract share the extremes of the Y axes. Besides that, the color of a time series is given by the color used on the corresponding Compact Spatial Abstract (i.e., matrix plot).

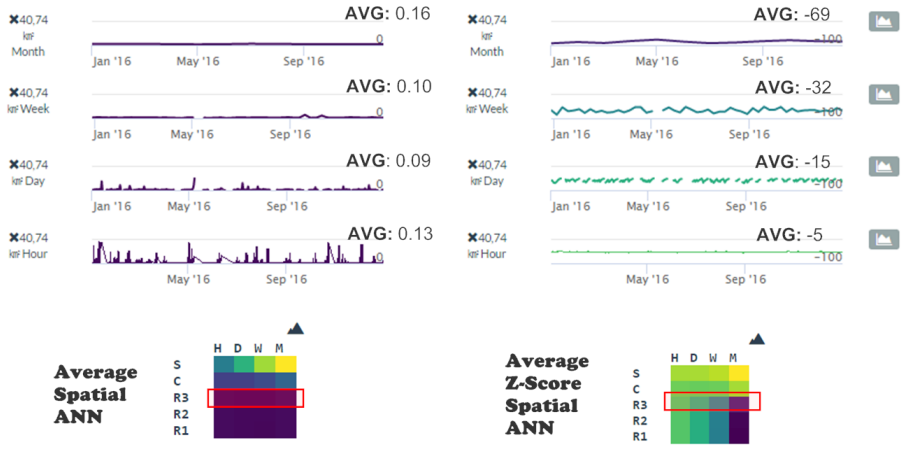

Fig. 9 The Spatial Average nearest neighbor and its z-score in four st-LoD.

Recall that, if the value of the Spatial ANN is less than 1, the trend is toward spatial clustering while if the value is greater than 1, the trend is toward dispersion. Very low or very high z-score values suggest some spatial pattern, and therefore, we can reject the complete spatial randomness.

Based on Fig.9, the Spatial Abstracts revealed a clustered phenomenon over time, since the average of the Spatial ANN values points to clusters of events throughout time. In the st-LoD - $(R3, Hours)$ we can observe variations between a clustered and a non clustered phenomenon. But in the remaining st-LoD, the phenomenon reveals to be quite stable and clustered because the values of the Spatial ANN are constantly close to zero and the corresponding z-scores are quite negative (i.e., the z-score is not close to zero).

As these two Spatial Abstracts complement each other, we plot them in a scatter plot, using the interface (a click on the right-side buttons displayed in Fig. 9). These scatter plots are displayed in Fig. 10. Notice that, the extremes on both axes are relative to the st-LoD shown. Each point in a scatter plot shows the values of the two Spatial Abstracts that occurred at a particular temporal granule. Therefore, the number of points in a scatter plot is equal to the number of temporal granules in the temporal granularity that composes the st-LoD being displayed.

At the st-LoD - $(40,74km^2, Hour)$, there are many points holding a value close to zero of the Spatial ANN, and their z-scores are not so negative as the ones in the others st-LoD. Looking at the st-LoD - $(40,74km^2, Month)$, it seems that the

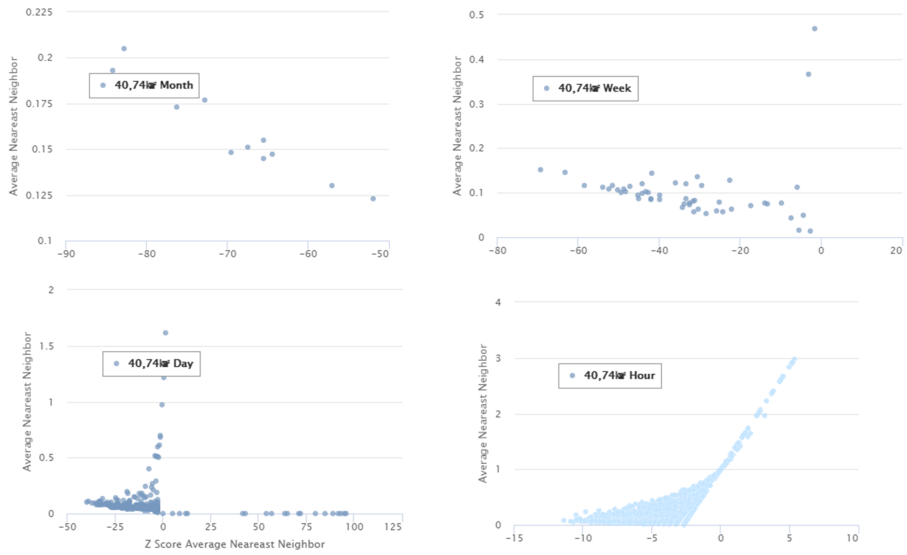

Fig. 10 The Spatial ANN and its Z-score displayed in four st-LoD.

phenomenon is always clustered (i.e., the values of Spatial ANN are close to zero and their z-scores quite negative). Finally, regarding the st-LoD - $(40, 74km^2, Day)$ and st-LoD - $(40, 74km^2, Weeks)$ seems to be the st-LoD that better fit the Poisson Cluster process. Recall that, in a Poisson Cluster process, events occur near other events but there are a few times where no events occur. This is visible in the scatter plots of the st-LoD - $(40, 74km^2, Day)$ and st-LoD - $(40, 74km^2, Weeks)$, once the majority of the points have the values of the Spatial ANN close to zero and their z-scores are quite negative. However, there are also points where the values of the Spatial ANN are close to zero and their z-scores are positive (no clustering) and also there are points with values of the Spatial ANN that are far from zero (no clustering).

In short, the analysis made over Dataset 2 that contains a Poisson cluster process simulated with clusters of events dispersed within 110 km and one day around their parents was:

- We use the matrix plots to analyze the GMBN, *Occupation rate* and *Collision rate*. Here, the GMBN pointed to the st-LoD - $(R3, Days)$
- We correlate the GMBN and Collision rate using the correlation of evolution through spatial granularities and through temporal granularities. Again, the st-LoD - $(R3, Days)$ was suggested.
- We used the phenomenon representation area to have an overview of the phenomenon at st-LoD - $(R3, Days)$ in three temporal granules chosen without any particular criterion. Clusters of events were observed.
- The Temporal Abstract - Temporal Center Masss Positioning was studied in three different LoDs. Furthermore, two Compact Temporal Abstracts were also analyzed: Coefficient of variation and the spatial autocorrelation. Here, the st-LoD suggested was also st-LoD - $(R3, Days)$ if one wants to understand in what periods of time clusters of events occur in certain geographic regions. It

was also possible to observe that the clusters are spread out over the entire area of the USA.
- The Spatial Abstracts - Spatial average nearest neighbor (Spatial ANN) and its z-score was used to understand not only when the clusters are happening but also what st-LoD better fits the Poisson Cluster process. The analysis suggested that clusters are distributed throughout the one "year" in which data was simulated. Finally, the analysis suggests that the st-LoD that better fits the Poisson Cluster process is st-LoD - $(R3, Days)$ or $(R3, Weeks)$.

Other datasets were simulated following the Poisson cluster model - the Datasets 3, 4 and 5. These datasets were simulated within the USA boundaries over a year. In **Dataset 3**, each cluster of events was built around a parent within a spatial distance of 2 km and a temporal distance of one week. **Dataset 4** is similar to Dataset 2 but contains an additional 3.000 events following a homogeneous model. These 3.000 events are spread out over the same period of the 30.000 events that follow the Poisson Cluster model. Finally, in **Dataset 5**, each cluster of events was built around a parent within a spatial distance of 570 km and a temporal distance of one week. In the following analysis, we also add Dataset 1 that was simulated with the Homogeneous model.

The datasets described were also modeled using similar valid granularities. All the granularities are equal with respect to the previous demonstration case except for the Raster granularities. This occurs because the minimum bounding box made by the events of the phenomenon might change from one dataset to another. Nevertheless, the most detailed spatial granularity is based on a grid of 16384 x 16384 cells and the other coarser spatial granularities were obtained by dividing the grid by a factor of 4.

Datasets 1, 3, 4, 5 will be discussed more briefly, discussing if whether the *VAST* points to suitable LoDs to detail our analyses once the "detailed" analyses would be similar to the ones made over Dataset 2. Furthermore, a comparison between the abstracts' values obtained by a Poisson Cluster dataset or a Homogeneous dataset is made.

Fig. 11 shows the global abstracts for all spatiotemporal LoDs of datasets 1, 3, 4 and 5. First of all, the *Occupation rate* follows a similar pattern in all datasets. Dataset 3 stands out from the others regarding the Collision rate. This occurs because the clusters in Dataset 3 were simulated within a spatial distance of 2 km, and were thus much more spatially clustered than in the other datasets. As a result, the collision among granular syntheses starts to occur "sooner", i.e., in finer st-LoDs when compared to the other datasets.

As to Dataset 3, the GMBN highlights the following st-LoDs:

1. $(Raster(0.1km^2), Days)$;
2. $(Raster(0.1km^2), Weeks)$;
3. $(Raster(1.6km^2), Days)$;
4. $(Raster(1.6km^2), Weeks)$

In this case, the values of spatiotemporal interaction are similar among the four st-LoDs, and therefore, any of the st-LoDs highlighted is potentially suitable to detail our analyzes. Nevertheless, the st-LoDs - $(Raster(1.6km^2), Weeks)$ is the st-LoDs that better approaches the st-LoDs in which the data was simulated, once each cluster of events was simulated around a parent within a spatial distance of 2 km and a temporal distance of one week.

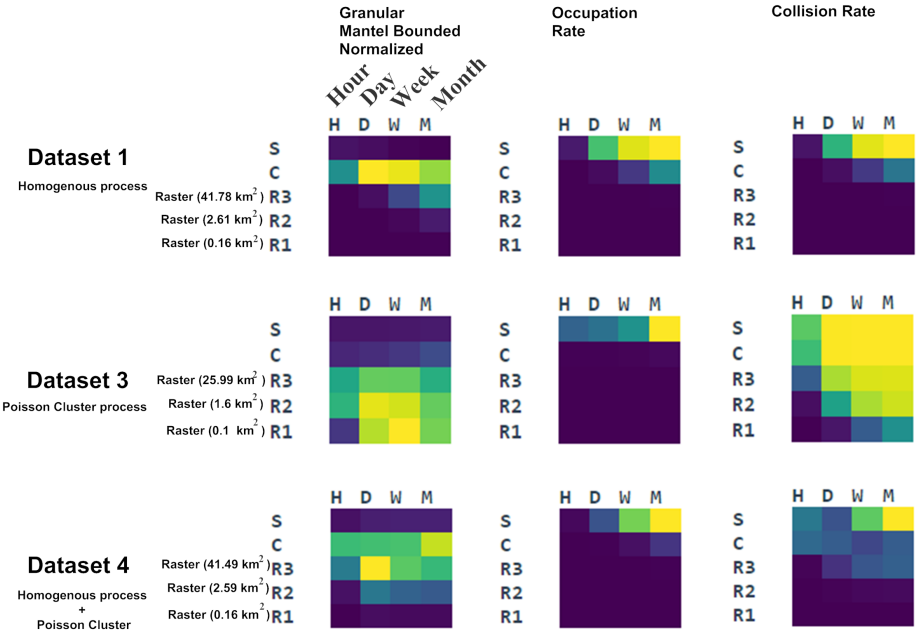

Fig. 11 Global Abstracts regarding Dataset 1, 3, 4.

Dataset 4 is similar to Dataset 1, complemented by a homogeneous process. In this case, the GMBN suggest the st-LoDs - $(Raster(41.49km^2), Days)$, which is the st-LoDs that better approaches the st-LoDs in which the pattern is simulated, once each cluster of events was simulated around a parent within a spatial distance of 110 km and a temporal distance of one day.

Nevertheless, a single Global Abstract should not be used to immediately guide our analyses for one or more st-LoDs. So far, we have been using four global abstracts to have a grasp of the data. From these four abstracts, one is neighborhood dependent (GMBN) and the remaining ones are not (*Occupation rate*, *Reduction rate*). In other words, only the GMBN captures in their computation the spatiotemporal dynamics of events. Therefore, restricting ourselves to just one global abstract that looks for spatiotemporal patterns or properties of the spatiotemporal interaction might wrongly suggest one or more st-LoDs as demonstrated below.

In Dataset 5, the GMBN highlights the following st-LoDs: (i) $(Counties, Hours)$; (ii) $(Counties, Days)$. However, each cluster of events was simulated around a parent within a spatial distance of 570 km and a temporal distance of one week. The problem is that the events within a cluster are spatially "dispersed" (570 km) and the GMBN is not capable of capturing such situation. In Dataset 1, the st-LoDs - $(Counties, Days)$ and $(Counties, Weeks)$ are pointed as potential st-LoDs in which there might be spatiotemporal interaction. However, this dataset was generated following a Homogenous model. This kind of scenarios can be easily discarded when we analyze several Global Abstracts that are looking for spatiotemporal patterns, or Global Abstracts with Compact Spatial Abstracts, or Global Abstracts with Compact Temporal Abstracts, or even all together.

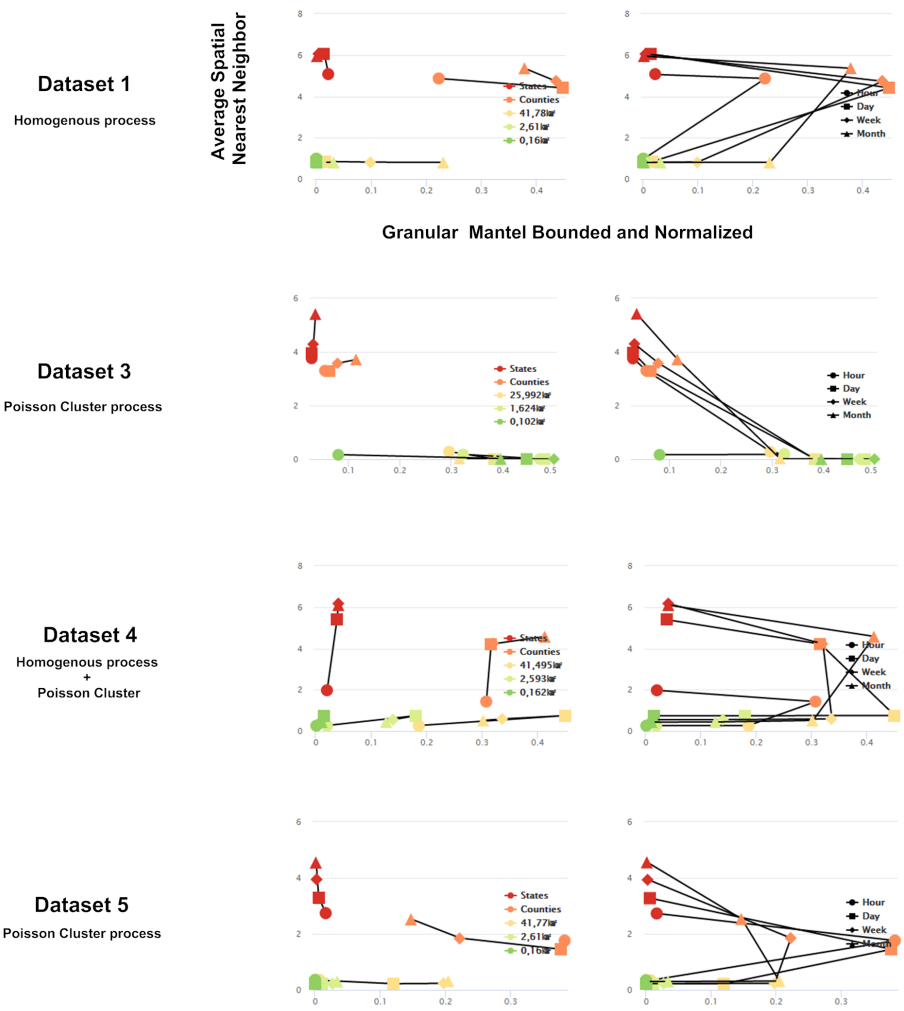

Fig. 12 Correlation between the GMBN and the Average of the Spatial ANN (Compact Spatial Abstract).

To illustrate the previous idea, we analyzed the correlation between the GMBN and the Average of the Spatial ANN (Compact Spatial Abstract) for the different datasets as displayed in Fig.12.

Let's consider Dataset 1 that is the one with the Homogeneous process. The correlation charts shows that when the GMBN reaches its maximum value, the value of the Average of the Spatial ANN is much greater than 1 (squared orange marker). Therefore, this phenomenon follows hardly a clustered pattern over time because in that case the value of the Average Spatial ANN would be closer to 0, something that did not happen in any st-LoDs as the minimum value achieved was 0.8.

In Dataset 3, we have a clear hint about the st-LoDs where the pattern was simulated because when the GMBN reaches its maximum value the Average of the Spatial ANN is close to zero (diamond green marker), as opposed to what happens in Dataset 1 (see Fig.12).

Looking at Dataset 4, the most pronounced "elbow" tip in the chart on the left (yellow square marker) corresponds to the st-LoD - $(Raster(41.49km^2), Days)$. This st-LoDs is the one that better approaches the st-LoDs in which the pattern was simulated, because each cluster of events was simulated around a parent within a spatial distance of 110 km and a temporal distance of one day. Despite the fact that GMBN reaches it's maximum in the yellow square st-LoD - $(Raster(41.49km^2), Days)$, the value for the Average of Spatial ANN is 0.5 which makes the hint weaker than in the case of Dataset 3. However, this gives us a clue for the right st-LoDs.

Regarding Dataset 5, we do not have a clear hint about the st-LoDs in which the data should be analyzed. Recall that, in this dataset, each cluster of events was simulated around a parent within a spatial distance of 570 km and a temporal distance of one week. So, the events are not that clustered. Therefore, the pattern is not so pronounced when compared with the other datasets. That being said, when the GMBN reaches its maximum value the Average of the Spatial ANN is **not** close to zero (square and circle orange markers - the st-LoD - $(Counties, Hours)$ and $(Counties, Days)$). This result has similarities with Dataset 1 - Homogeneous process. However, in this case, two "elbow" tips are observed (i.e., st-LoD) that are not so pronounced but the Average Spatial ANN is close to zero. These correspond to the st-LoD - $(Raster(41.77km^2), Weeks)$ (i.e., the diamond yellow marker) and $(Raster(41.77km^2), Months)$ (i.e., the triangle yellow marker). In this case, the SUITE-VA provide a hint about two st-LoD such that one of them (i.e., st-LoD - $(Raster(41.77km^2), Weeks)$) may be appropriate to detail further analyzes. The previous analysis would not be as clear for an user that is unfamiliar with the abstracts implemented as well as the interpretation of the visualizations provided. This relates to the learning curve concept. As a user is gaining more experience with the *VAST*, the understanding about the concepts involved will also become clearer.

A final remark about the interpretation of the correlation charts. The "elbow" tips provide a change from a positive to a negative (or vice-versa) correlation that might be interesting to explore. Nevertheless, there might be st-LoD of interest that do not correspond to "elbow" tips. Yet, according to the values that they hold for the abstracts at study, they might be also interesting to explore as in Dataset 5.

5.1.2 Contagious Process

Dataset 6 was simulated following the contagious process. The dataset was simulated within the USA boundaries over a year and is composed of 5.000 events. Based on an initial event, the next ones are generated within a spatial distance of 110 km and a temporal distance of a week. Furthermore, the dataset was modeled through the *synthetic* predicate. In this case, the most detailed spatial granularity $Raster\left(0.05km^2\right)$ is based on grid of 16384 x 16384 cells that cover the analyzed spatial extent of the phenomenon, and each cell has an area of $0.05km^2$. The other coarser spatial granularities were obtained by dividing the number of cells in the

grid by a factor of 4. So the valid granularities for space were rasters with cell sizes approximately of $0.05km^2$, $0.8km^2$, and $12.5km^2$. The granularities *Counties* and *States* were also included. The time granularities used were $Hours$, $Days$, $Weeks$, $Months$.

To start our analysis we chose: (*i*) the GMBN; (*ii*) the Average of Spatial ANN; (*iii*) the Average of the z-score of the Spatial ANN; (*iv*) the Average of Temporal ANN; (*v*) the Average of the z-score of the Temporal ANN. The first three abstracts were already used so we skipped more explanations.

The Parallel Coordinates was used to simultaneously analyze the global abstracts chosen across all the st-LoDs. In this case, we are interested in understanding st-LoDs in which (*i*) the phenomenon seems to be more clustered over time; (*ii*) the phenomenon seems to be more clustered over space; (*iii*) the st-LoDs where the spatiotemporal interaction of events seems to be better perceived. To conduct such analysis, we filtered the Parallel Coordinates in each coordinate.

This way, interactively, we just considered st-LoDs with values below 0.4 (approximately) regarding the average of the Spatial ANN. For the average of its z-score, we just considered values below -10 (approximately). Furthermore, values below 0.1 (approximately) with respect to the average of the temporal ANN were considered. For its z-score, we considered values below -1. Finally, the top three values of the GMBN were considered, which means values above 0.08. The results are displayed in Figure 13.

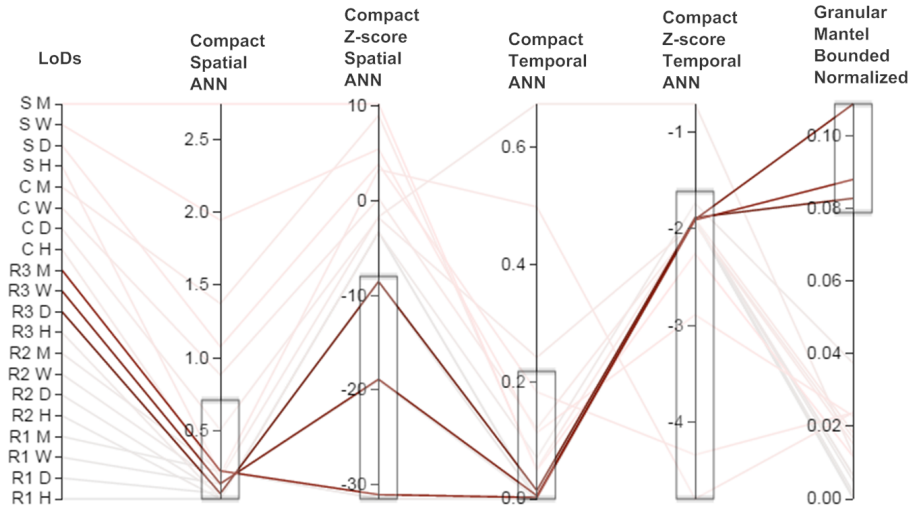

Fig. 13 Overview of the Dataset 6 using Global Abstracts, Compact Spatial Abstracts and Compact Temporal Abstracts.

Three st-LoDs were highlighted:

1. $(12.5km^2, Days)$;
2. $(12.5km^2, Weeks)$;
3. $(12.5km^2, Months)$

Like it was done in Dataset 2, the Temporal Center Mass's Positioning was used to relate geographic regions with the center's of mass of time at which events happened. This Temporal Abstract is displayed in Fig. 14 for the three st-LoDs identified. Regardless of the st-LoD, a grasp about the spatial path made by the

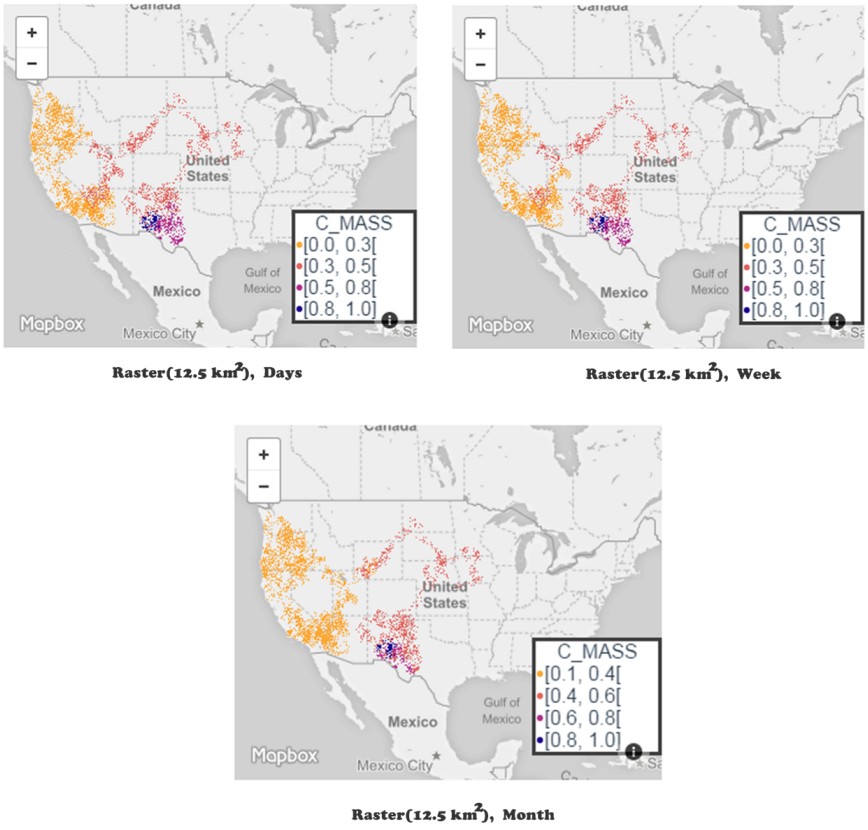

Fig. 14 One Temporal Abstract at three different st-LoDs.

simulated contagious process is visible, thus confirming a contagious process. Nevertheless, in st-LoD - $(12.5km^2, Days)$ is where the path made is slightly better perceived.

Another experiment was made with two Spatial Abstracts: (i) the Spatial Scope; (ii) the Spatial Consecutive Distance between Centers of Mass. The former abstract indicates how much a phenomenon changes the size of its spatial extent over time while the latter measure whether such spatial extent moves in space over time. For the st-LoD identified initially, the Spatial Abstracts can be seen in Fig. 15. Moreover, in the former abstract the average value is displayed while in the latter the coefficient of variation is shown.

Let's start by the Spatial Scope. In general, for the st-LoD identified, the phenomenon's spatial scope is quite stable throughout time with some variations here and there. However, the most stable st-LoD is the $(Raster(12.5km^2), Months)$.

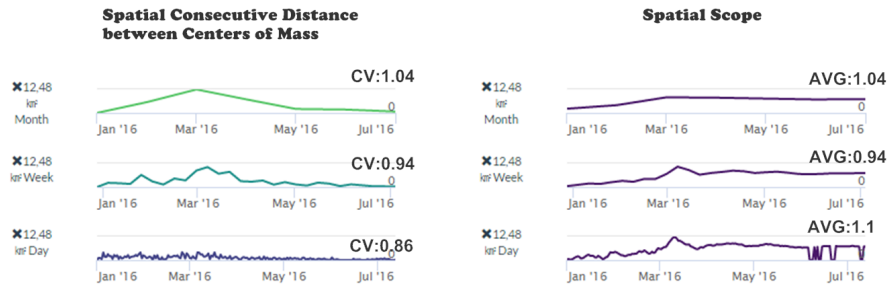

Fig. 15 Two Spatial Abstracts about Dataset 6.

Regarding the Spatial Consecutive Distance between Centers of Mass, st-LoD - $(Raster(12.5km^2), Days)$ is where the distances between centers of mass seem to vary less according to the coefficient of variation. Thus, if one is interested in understanding how the contagious process evolved, in this simulated scenario, one should look at the st-LoD - $(Raster(12.5km^2), Days)$ because this is the st-LoD that seems to capture the smoothest transitions over time.

To conclude, in the Contagious process an initial event is generated, and then, the next events are simulated within a specified spatial and temporal distance. The dataset under analysis was generated with distances of 110 km and one week. The events generated within neighborhood are uniformly distributed and they are not necessary at a distance of a week. In fact, many of them might be at temporal distance less than a week. This might explain why, in the st-LoD - $(Raster(12.5km^2), Days)$, the Contagious process seems to be better perceived.

5.1.3 Log-Gaussian Cox Process

Dataset 7 was simulated following the Log-Gaussian cox process. The dataset was simulated within the USA boundaries over a year and is composed by 15.000 events. Therefore, this dataset will show geographic regions of higher incidence of events over others.

In this case, the most detailed spatial granularity R1 is based on grid of 16384 x 16384 cells that cover the analyzed spatial extent of the phenomenon, and each cell has an area of $0.16km^2$. The remaining valid raster granularities for space were $2.57km^2$, and $41.27km^2$. The granularities $Counties$ and $States$ were also included. The time granularities used were $Days$, $Weeks$, $Months$.

As in Dataset 6 (Contagious process), we start by getting an overview of the set of the following abstracts using the Parallel Coordinates: (i) the GMBN; (ii) the average of Spatial ANN; (iii) the average of the z-score of the Spatial ANN; (iv) the average of temporal ANN; (v) the average of the z-score of the temporal ANN. Looking at the Parallel Coordinates:

– There are no st-LoDs holding values close to zero with respect to **Average Spatial ANN** containing quite negative z-scores. This kind of values suggest that we are not dealing with the Poisson cluster process as events occur close to each other in space.

– There are some st-LoDs holding values close to zero with respect to Average Temporal ANN but their z-scores are also close to zero. Also, for such cases, the spatiotemporal interaction is weak when compared with other st-LoDs. This kind of values suggests that we are not dealing with the Contagious process as events occur close to each other in space and in time.
– Two st-LoDs have the spatiotemporal interaction among events measured by the GMBN above 0.4, which is similar to the values obtained in Poisson Cluster simulated datasets. However, at this point, no particular meaning can be assigned to such values.

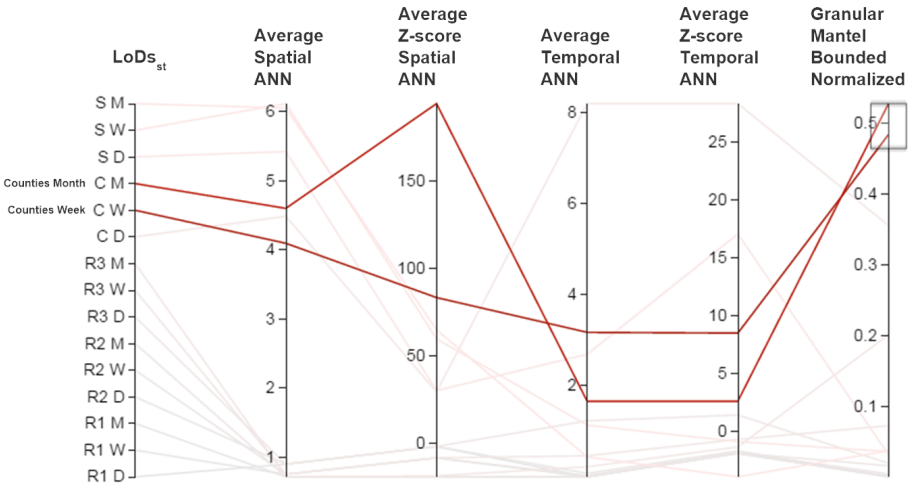

Fig. 16 Overview of the Dataset 7 (Log-Gaussian cox process) using Global Abstracts, Compact Spatial Abstracts and Compact Temporal Abstracts.

In Log-Gaussian Cox processes, we have geographic regions of higher incidence that might change slowly over time. This way, there are geographic regions that distinguish themselves from others in terms of the number of events that happened in there as well as the geographic regions of higher incidence that might "infect" their neighbors.

Since Log-Gaussian Cox processes simulated geographic regions of higher incidence, temporal abstracts might be useful. Hence, we chose the **Temporal Frequency Rate** that measures for each spatial granule the percentage of atoms occurred on it given all the atoms of the phenomenon at a given LoD. To capture the st-LoD where the Log-Gaussian Cox process is better perceived, we correlate the Compact Temporal Abstract - Coefficient of variation and the Spatial autocorrelation of the Temporal frequency rate as can be seen in Fig. 17. These two Compact Temporal Abstracts are chosen because, we want to capture the st-LoDs in which there is a considerable variation on the Temporal frequency rate, and simultaneously, to understand whether the spatial granules are spatially correlated on the Temporal frequency rate.

First of all, the temporal granularity does not have an impact on the **Temporal Frequency Rate**. Regardless the temporal granularity, the percentage of atoms

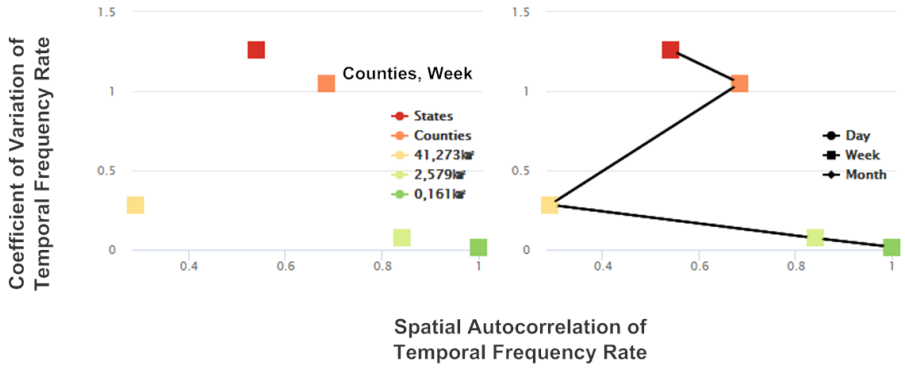

Fig. 17 Dataset 7 (Log-Gaussian Cox process) - Correlation between the Coefficient of Variation of Temporal Frequency Rate and the Spatial Autocorrelation of Temporal Frequency Rate.

occurred on particular spatial granules remains the same as can be observed on the left chart of Fig. 17.

That being said, let's focus on the right chart in Fig. 17. In finer spatial granularities, a spatial autocorrelation among spatial granules it is expected to exist, once their values diverge little or nothing as shown by their coefficient of variation. But when we look at the st-LoD - $(Counties,\ Week)$, the coefficient of variation is a value near to one, which indicates variability among values, and simultaneously, the level of spatial autocorrelation grows. But if we move to st-LoD - $(States,\ Week)$, the spatial autocorrelation decreases. To check the previous analysis, the **Temporal Frequency Rate** is shown in Fig. 18 at the st-LoD - $(Counties,\ Week)$.

There are some counties (that are spatially small) on the east side of USA (highlighted with a red arrow) that have a greater incidence of events. Such geographic area was zoomed-in and displayed at two st-LoDs: (i) $(Counties,\ Week)$; (ii) $(Raster\left(41.27km^2\right),\ Week)$ as shown in Fig. 19.

Looking at the st-LoD - $(Raster\left(41.27km^2\right),\ Week)$ geographic regions with higher incidence of events are no longer perceived. Although there are geographic regions with higher incidence (purple and dark blue spatial granules), the values of **Temporal Frequency Rate** are not different as they are in the st-LoD - $(Counties,\ Week)$. This confirms that the st-LoD - $(Counties,\ Week)$ is probably one of the suitable st-LoD to better understand the geographic regions that are most affected by the phenomenon.

5.2 Real Datasets

Several phenomena were analyzed using the *VAST*. As opposed to synthetic datasets, we are not aware of possible patterns that those phenomena might contain.

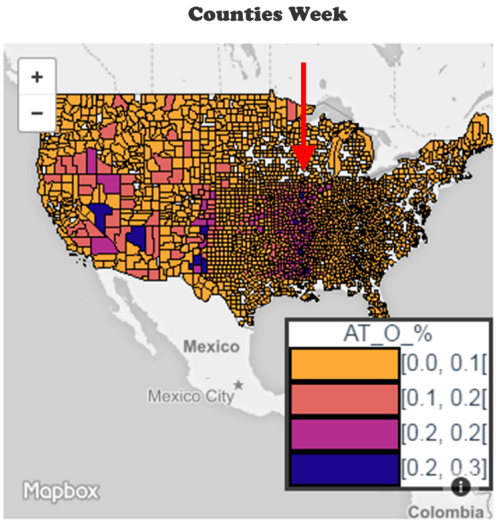

Fig. 18 The **Temporal Frequency Rate** at the st-LoD - (*Counties*, *Week*)

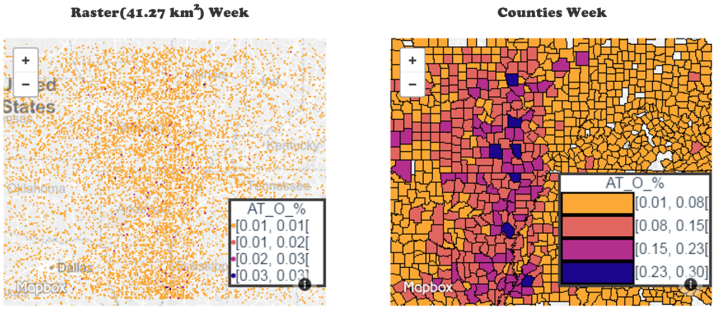

Fig. 19 The **Temporal Frequency Rate** at the st-LoD - (*Raster* $\left(41.27km^2\right)$, *Week*) and (*Counties*, *Week*).

5.2.1 Wildfires in Portugal

Here, we report the analysis made about wildfires that occurred in Portugal between 2001 and 2012.

The following pages shows the analysis made about wildfires that occurred in Portugal between 2001 and 2012. The granularities-based model was used to model them at different LoDs. This phenomenon is described by a collection of 280.968 spatiotemporal events. These events were modeled through the wildfires predicate containing two arguments $wildfires(space, time)$.

The most detailed spatial granularity *Raster* $\left(0.005km^2\right)$ is based on grid of 16384x 16384 cells that cover the analyzed spatial extent of the phenomenon, and each cell has an area of 0.005 km^2.

The remaining raster granularities for space were granularities with cell sizes of 0.08 km^2 and 0.319 km^2. The granularities *Parishes*, *Counties* and *Districts* was

also considered. The time granularities used were $Hours$, $Days$, $Weeks$, $Months$, $Years$.

The considered granular terms required to model these events were: $Instant$ and $Cell$ for the time and space arguments, correspondingly. The raw data were encoded at the at the finer st-LoD, which includes the time granularity of $Hours$ and the space granularity $Raster\ (0.005km^2)$.

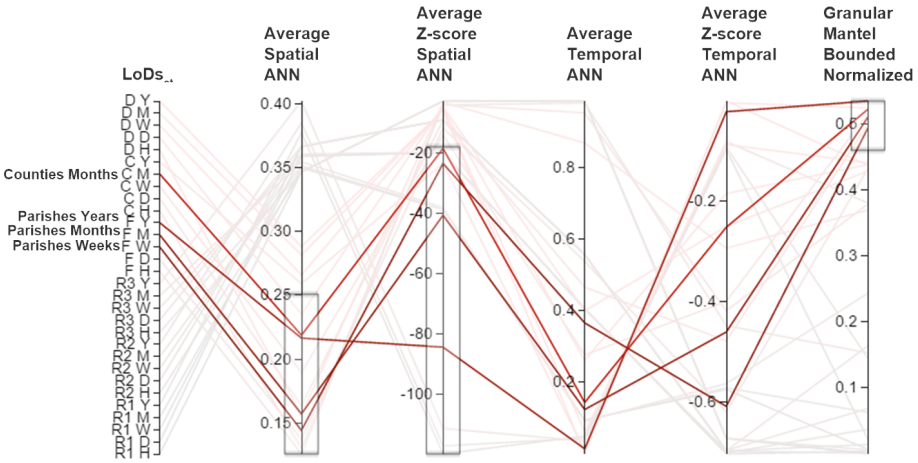

Fig. 20 Overview of wildfires in Portugal using Global Abstracts, Compact Spatial Abstracts and Compact Temporal Abstracts.

To have a grasp of wildfires in Portugal, we chose the following abstracts: (i) the GMBN; (ii) the average of Spatial ANN; (iii) the average of the z-score of the Spatial ANN; (iv) the average of Temporal ANN; (v) the average of the z-score of the Temporal ANN. The Parallel Coordinates was used to simultaneously analyze the global abstracts chosen across all the st-LoDs. Let's take a close look at them.

- There are st-LoDs holding values close to zero with respect to Average Spatial ANN that simultaneously have quite negative values considering its z-score. Therefore, this kind of values have some resemblances with the ones obtained with Poisson cluster simulated datasets or the Contagious ones. As a result, at this point, we might say that wildfires in Portugal hardly follow a homogeneous model.
- Several st-LoDs are holding values close to zero with respect to Average Temporal ANN but their z-scores are close to zero, which means that the complete randomness cannot be rejected. In other words, wildfires occurring on the same spatial granule are likely not close to each other in time, on average. Furthermore, this information is telling us that probably, we are not dealing with a phenomenon that follows a Contagious process.
- Several st-LoDs have the spatiotemporal interaction among events measured by the GMBN above 0.4, which is similar to the values obtained in Poisson Cluster simulated datasets. This reinforces the similarities of the wildfires in Portugal with the Poisson Cluster model.

Based on the preliminary analysis, wildfires in Portugal seem to approach the Poisson Cluster model. The Parallel Coordinates was filtered to identify the suitable st-LoDs to confirm the previous hypothesis. We just considered st-LoDs with values below 0.25 (approximately) regarding the Average of the Spatial ANN. For the average of its z-score, we just considered values below -20 (approximately). Finally, the top four values of the GMBN were considered, which means values above 0.45 (approximately). The other coordinates (temporal average nearest neighbor and its z-score) were not filtered because there are no domain values that clearly points to clustered or dispersed events in time. From the filtering conducted, four st-LoDs were highlighted: $(Parishes, Weeks)$, $(Parishes, Months)$, $(Parishes, Years)$, $(Counties, Months)$.

To better understand how wildfires, occur in space over time, the Spatial ANN and its z-score were plotted in a scatter plot for the st-LoDs identified previously as can be seen in Fig. 21. First of all, notice that, the charts obtained present similarities in the values and corresponding "shapes" with the charts obtained when we studied Poisson Cluster simulated datasets. Furthermore, in all st-LoDs displayed, the phenomenon reveals to have several clustered distributions of events over time.

Nevertheless, st-LoDs (chart on the bottom-right) is the one that better fits the Poisson Cluster process/model. That is, in general, events occur near one another but there are a few times when events did not occur or occur in a dispersed way. Furthermore, in the st-LoDs - $(Parishes, Weeks)$ there is a good trade-off between the Spatial ANN and its z-score. In other words, there are many temporal granules in which the Spatial ANN's values are around 0.15 (trend toward clustering) and where their z-scores are quite negative (confirmation of clustering).

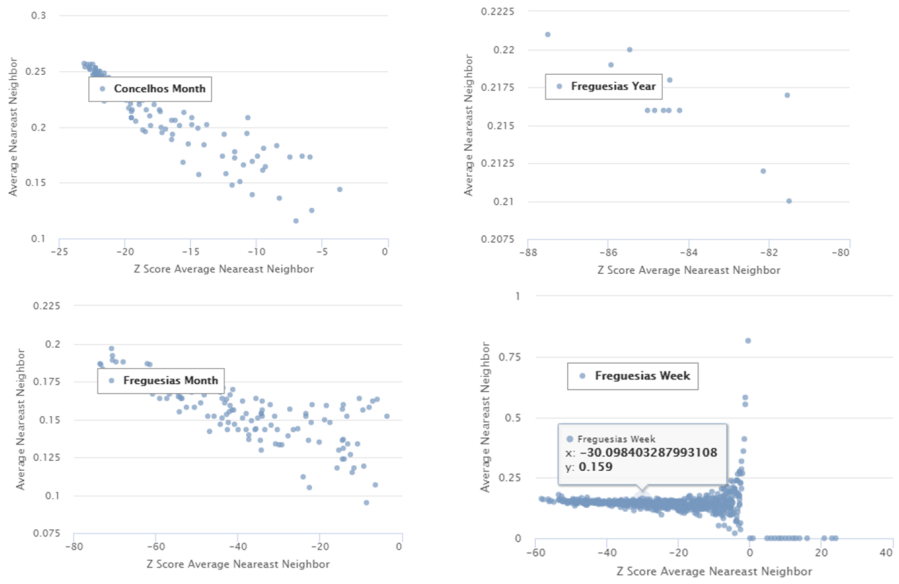

Fig. 21 The Spatial ANN and its Z-score displayed in four st-LoDs.

VAST tool allows users to zoom-in on a particular area of a scatter plot. When that action is performed the selected points (i.e., temporal granules) are highlighted on the corresponding time-series using vertical red lines. Thus, to understand when wildfires are occurring spatially clustered, we zoom-in the scatter plot at st-LoDs - $(Parishes, Weeks)$ over the area where the Spatial ANN is less than 0.2 and its z-score is less than -35. So, we are choosing the temporal granules in which the events are more spatially clustered. The result of this selection can be seen Fig. 22.

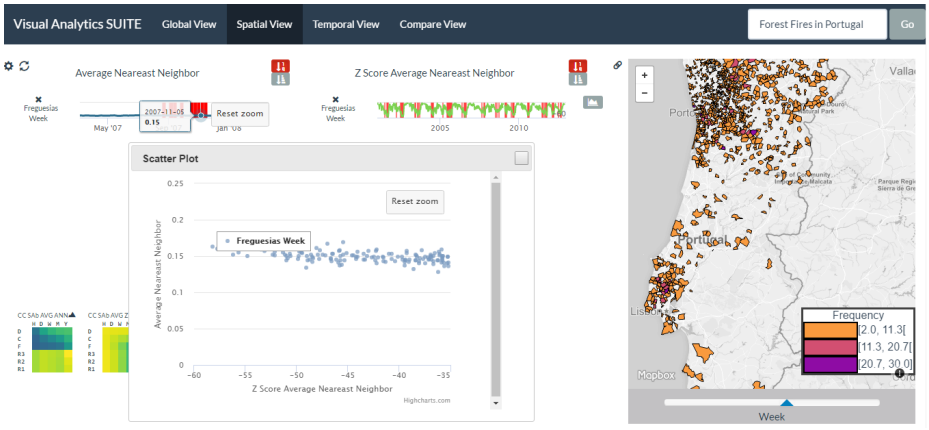

Fig. 22 Filter the temporal granules in which the clusters of events are most pronounced at st-LoDs - $(Parishes, Weeks)$.

The time series on the right-hand side is showing the entire temporal period at study. From it, we can notice that the wildfires occurred recurrently spatially clustered which, in general, matches the summer periods but not necessarily. For instance, during the week that has started on November, 5^{th} 2011, several wildfires occurred in Portugal. These are displayed on the map of Fig. 22, and it is possible to confirm that they are spatially clustered.

5.2.2 Violence against Civilians

This section shows the analysis made over violence against civilians in Africa that occurred between 1997 and 2015. The granularities-based model was used to model them at different LoDs. This phenomenon is described by a collection of 33.393 spatiotemporal events. These events were modeled through a terrorism predicate, with two arguments $terrorism(space, time)$.

The most detailed spatial granularity $Raster\ (343.45km^2)$ is based on a grid of 16384 x 16384 cells that cover the analyzed spatial extent of the phenomenon, and each cell has an area of 343.45 km^2. The other coarser spatial granularities were obtained by dividing the number of cells in the grid by a factor of 2. So the valid granularities for space were rasters with cell sizes of 1376.34 km^2, 5525.79 km^2, and 22268.15 km^2. The used time granularities were $Hours$, $Days$, $Weeks$, $Months$, $Years$.

Like previously, we start by trying to figure out what kind of model might be underlying this phenomenon using the usual abstracts: (*i*) the GMBN; (*ii*) the Average of Spatial ANN; (*iii*) the Average of the z-score of the Spatial ANN; (*iv*) the Average of Temporal ANN; (*v*) the Average of the z-score of the Temporal ANN. The Parallel Coordinates are displayed in Figure 23.

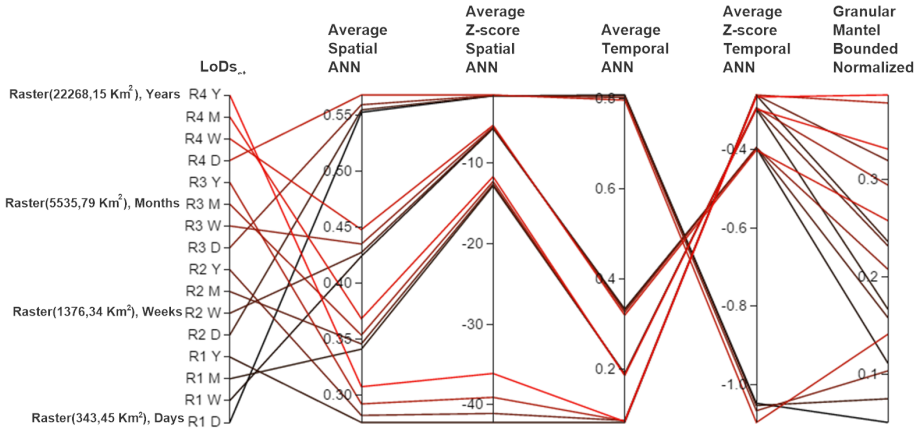

Fig. 23 Overview of the attacks against civilians in Africa using Global Abstracts, Compact Spatial Abstracts and Compact Temporal Abstracts.

There are "four levels" of spatial clustering over time as depicted by the Average Spatial ANN and the corresponding z-scores. These levels are being strongly influenced by the temporal granularity. With the granularity $Years$, the Average Spatial ANN and the corresponding z-scores reach their minimums while with the granularity $Days$ the spatial clustering over time is not so pronounced. Thus, the phenomenon seems to have some similarities to the Poisson Cluster model.

Several $LoDs_{st}$ are holding values close to zero with respect to Average Temporal ANN but their z-scores are also close to zero, which means that the complete randomness cannot be rejected. In other words, the attacks against civilians occurring on the same spatial granule are likely not close to each other in time, on average. Furthermore, this information is telling us likely, we are not dealing with a phenomenon that follows a Contagious process. This is quite similar to the phenomenon about Wildfires in Portugal.

There are some $LoDs_{st}$ that have the spatiotemporal interaction among events measured by the GMBN above 0.3, which is similar to the datasets simulated with the Poisson cluster or with the dataset about wildfires in Portugal.

Since the Average Spatial ANN and the corresponding z-scores reach their minimums, we look to the data at the $LoDs_{st}$ - $(Raster(22268.15\ km^2),\ Years)$ in three temporal granules: 2008, 2009, 2010. The temporal granules were chosen for no particular reason but just to see if there were clusters of events based on the tip provided by the Parallel Coordinates (see Figure 23).

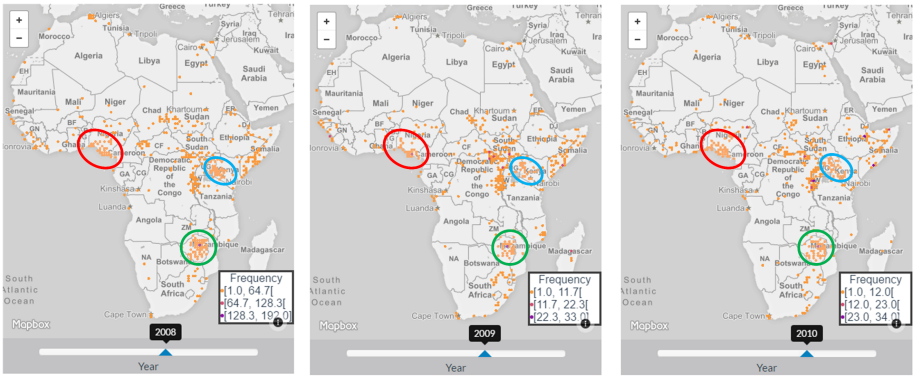

Fig. 24 Violence against Civilians at the $LoDs_{st}$ - $Raster(22268.15\ km^2)$, $Years$ displayed in three temporal granules - 2008, 2009 and 2010.

As we can see in Figure 24, the spatiotemporal events are in fact spatially clustered. In this case, there are clusters of events that remain stable in the three years chosen like for example the cluster in Mozambique (green circle), South Nigeria (red circle), and on the border between Uganda and Kenya (blue circle).

In our initial analysis about violence against civilians, the $LoDs_{st}$ containing the temporal granularity $Months$ also suggest some characteristics of the Poisson Cluster process, and consequently, clusters of events over time. So, we have chosen the $LoDs_{st}$ - ($Raster(22268.15\ km^2)$, $Months$) for displaying the Spatial ANN and the corresponding z-score. Afterward, we plot them in a scatter plot and filter out the temporal granules where the values of Spatial ANN are low and the values of the z-score are more negative, that is, the temporal granules where the clusters are likely most pronounced. This action highlights the time series on the respective granules as displayed in Figure 25.

Surprisingly, only "recent" temporal granules were highlighted which means that the attacks against civilians in Africa are getting more spatially clustered than in the past. A more detailed analysis about this change can be done and the $LoDs_{st}$ - ($Raster(22268.15\ km^2)$, $Months$) seems suitable for such an analytical task.

Another experiment was made to understand whether the attacks against civilians occur on the same regions over time or if there were changes. To conduct this analysis, we have chosen the Temporal Center Mass's Positioning. Since the spatial autocorrelation of the Temporal Center Mass's Positioning is most pronounced in $LoDs_{st}$ containing the spatial granularity $Raster(343.45\ km^2)$, our analysis was detailed in the $LoDs_{st}$ - $Raster(343.45\ km^2)$, $Weeks$. Some results were displayed in Figure 26.

Clusters of events are changing over time. For instance, in Angola most of the attacks occurred in the past and they are not that frequent anymore. The same is observed in Serra Leoa. But for instance, at northern Algeria, the attacks have slightly changed location over time from north-west to north-east. Looking at the north of Uganda (top right-hand map), there is no particular pattern, that is, in each spatial granule there may be old and recently attacks or the attacks happened

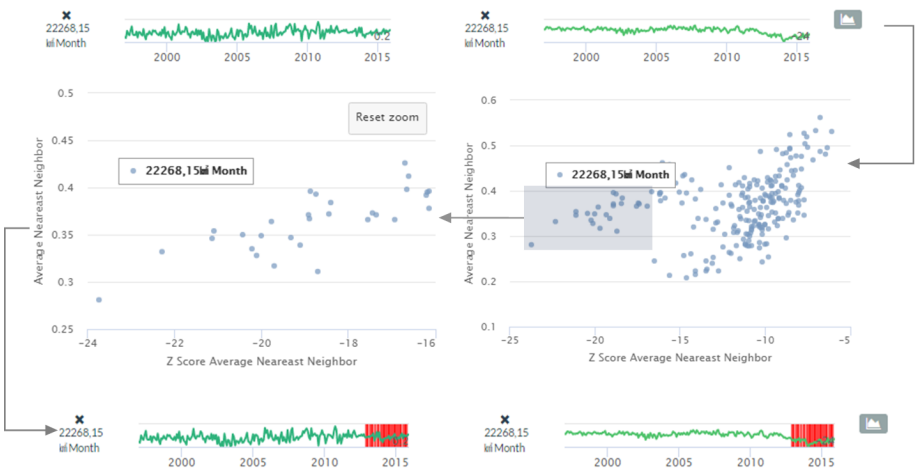

Fig. 25 Highlighting the temporal granules where the Violence against Civilians is more spatially clustered using the $LoDs_{st}$ - ($Raster$(22268.15 km^2), $Months$).

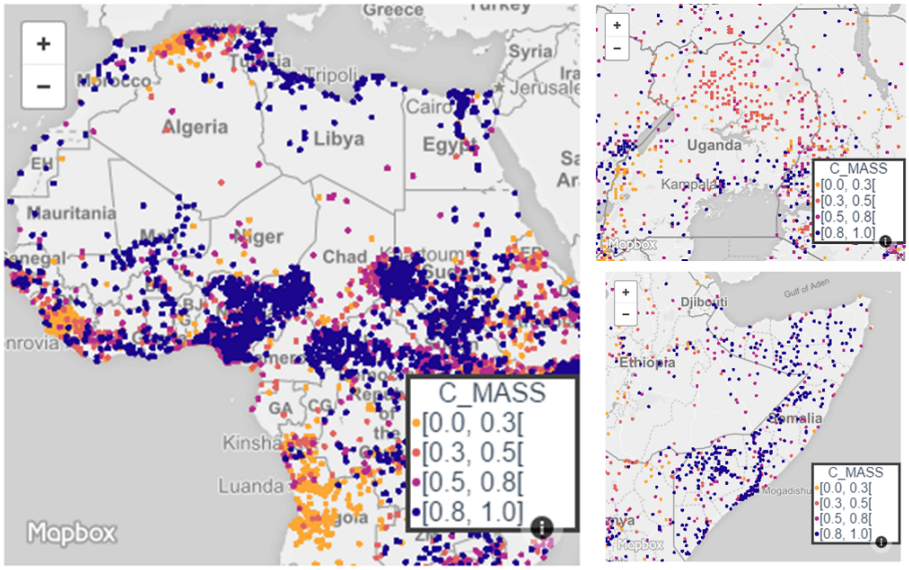

Fig. 26 Violence against Civilians at the $LoDs_{st}$ - $Raster$(343.45 km^2), $Weeks$ displayed in three different spatial extents.

somewhere in the middle of the period under study (1997-2015). At Somalia, most attacks are recent and spread out by the entire country.

In the case of Nigeria, we have used a feature of the *VAST*, which allows to hide and show the events holding a particular class of values. In Figure 27, from left to right, the classes were incrementally added to the map. As you can see, in the past, most attacks occurred at the south of Nigeria, and afterward, they started to spread across the entire country.

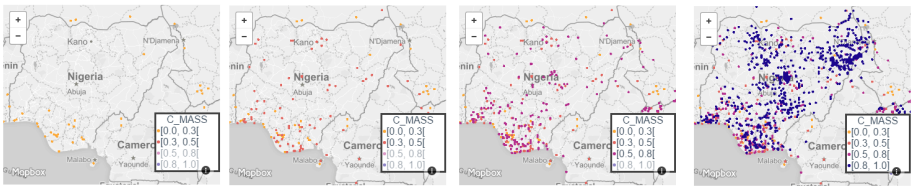

Fig. 27 Evolution of Violence against Civilians throughout time at the $LoDs_{st}$ - *Raster(343.45 km^2), Weeks* in Nigeria.

6 Conclusions and Future Work

The LoD plays a crucial role when analysing spatiotemporal data. From one LoD to another, some patterns can be perceived more easily, or different patterns may be detected. Modeling phenomena at different LoDs is needed, as there is no single LoD at which data can be analyzed.

Current practices work mainly on a single LoD, driven by the analysts' perception, ignoring the fact that identifying the suitable LoDs is key for pointing relevant patterns. To enhance the analyses over spatiotemporal events, we propose to move from a single user-driven LoD to a multiple LoDs analysis approach, providing the user with an understandable high-level overview of the underlying structure of the phenomenon for each LoD. This approach can give several hints about different facets of spatiotemporal events and give a first insight on the presence or absence of patterns at particular LoDs.

VAST was developed, to conduct analysis in this new mindset. The tool allows to visually inspect hints about the absence or presence of different spatiotemporal patterns at multiple LoDs, simultaneously, following a coordinated strategy among the visualizations provided.

The *VAST* tool is based on the Visualization of Abstracts, proposed within the scope of the SUITE framework, using an integrated set of visualizations including: parallel coordinates and matrix plots for the ST-Abstracts; linked temporal series for the Spatial Abstracts; linked maps for the Temporal Abstracts; a linked map with temporal sliders for the real data phenomena; and scatters for the correlation analysis for pairs of abstracts. In this paper we have demonstrated how the joint use of these visualizations allows the detection of many spatiotemporal patterns in the data and at which LoDs they are better perceived. We also proposed to use a new abstract, the Granular Mantel Bounded and Normalized (GMBN) abstract that measures the spatiotemporal interaction among granular syntheses. This abstract was very important in the process of patterns discovery.

To the best of our knowledge, there is no other prototype or application that supports the analysis of spatiotemporal events at multiple LoDs, simultaneously, following the VA Mantra.

Experiments were conducted with two types of datasets describing spatiotemporal events: (i) synthetic datasets; (ii) real datasets. Synthetic datasets with different spatiotemporal patterns (Poisson Cluster Process, Contagious Process, Log-Gaussian Cox Process) at different LoDs were produced. For most cases, VAST could provide a correct overview of the phenomenon allowing us to identify the LoDs where patterns exist and, therefore, the LoDs that should be used to detail the analysis. Two real datasets were analyzed and discussed: wildfires that oc-

curred in Portugal between 2001 and 2012; and violence against civilians in Africa that occurred between 1997 and 2015. In general, VAST was able not only to give an overview of the presence or absence of different spatiotemporal patterns but also to suggest the proper spatiotemporal LoDs that allow us to better perceive the corresponding patterns.

Future work can be directed for the development of heuristics to suggest automatically LoDs to analyze the data are needed and should be a priority because if the number of abstracts grows considerably it might be overwhelming to the user. This issue relates to the learning curve. Each abstract looks for a feature or pattern which frequently is expressed in terms of a range of values. According to the value, it means one thing or the other. Thus, a user needs to get familiar with the abstracts and their interpretation. Requiring a user to memorize all the abstracts and their interpretation might be overwhelming, specially if we consider the joint interpretation of abstracts. So again, heuristics to suggest automatically LoDs are needed.

References

Aigner W, Miksch S, Schumann H, Tominski C (2011) Visualization of time-oriented data. Springer Science & Business Media

Andrienko G, Andrienko N, Bak P, Keim D, Kisilevich S, Wrobel S (2011) A conceptual framework and taxonomy of techniques for analyzing movement. Journal of Visual Languages & Computing 22(3):213–232

Andrienko G, Andrienko N, Bosch H, Ertl T, Fuchs G, Jankowski P, Thom D (2013) Thematic patterns in georeferenced tweets through space-time visual analytics. Computing in Science & Engineering 15(3):72–82

Andrienko N, Andrienko G (2004) Interactive visual tools to explore spatio-temporal variation. In: Proceedings of the working conference on Advanced visual interfaces, ACM, pp 417–420

Andrienko N, Andrienko G (2006) Exploratory analysis of spatial and temporal data: a systematic approach. Springer

Bédard Y, Rivest S, Proulx MJ (2007) Spatial. online analytical. processing (solap): Concepts, architectures, and solutions. Data Warehouses and OLAP: Concepts, Architectures, and Solutions, Idea Group Inc pp 298–319

Bertin J, Berg WJ, Wainer H (1983) Semiology of graphics: diagrams, networks, maps, vol 1. University of Wisconsin press Madison

Box GE, Jenkins GM, Reinsel GC, Ljung GM (2015) Time series analysis: forecasting and control. John Wiley & Sons

Chae J, Thom D, Bosch H, Jang Y, Maciejewski R, Ebert DS, Ertl T (2012) Spatiotemporal social media analytics for abnormal event detection and examination using seasonal-trend decomposition. In: Visual Analytics Science and Technology (VAST), 2012 IEEE Conference on, IEEE, pp 143–152

Chen H, Chung W, Xu JJ, Wang G, Qin Y, Chau M (2004) Crime data mining: a general framework and some examples. Computer 37(4):50–56

Cho I, Dou W, Wang DX, Sauda E, Ribarsky W (2016) Vairoma: A visual analytics system for making sense of places, times, and events in roman history. IEEE transactions on visualization and computer graphics 22(1):210–219

Dykes J, MacEachren A, Kraak M (2005) Exploring geovisualization. No. vol. 1 in International Cartographic Association, Elsevier

Ebdon D (1985) Statistics in geography. Blackwell

Ferreira N, Poco J, Vo HT, Freire J, Silva CT (2013) Visual exploration of big spatio-temporal urban data: A study of new york city taxi trips. Visualization and Computer Graphics, IEEE Transactions on 19(12):2149–2158

Forlines C, Wittenburg K (2010) Wakame: sense making of multi-dimensional spatial-temporal data. In: Proceedings of the International Conference on Advanced Visual Interfaces, ACM, pp 33–40

Fuchs G, Schumann H (2004) Visualizing abstract data on maps. In: Information Visualisation, 2004. IV 2004. Proceedings. Eighth International Conference on, IEEE, pp 139–144

Gabriel E (2014) Estimating second-order characteristics of inhomogeneous spatio-temporal point processes. Methodology and Computing in Applied Probability 16(2):411–431

Gabriel E, Rowlingson B, Diggle P (2013) stpp: an r package for plotting, simulating and analyzing spatio-temporal point patterns. Journal of Statistical Software 53(2):1–29

Gatalsky P, Andrienko N, Andrienko G (2004) Interactive analysis of event data using space-time cube. In: Information Visualisation, 2004. IV 2004. Proceedings. Eighth International Conference on, IEEE, pp 145–152

Getis A (1992) The Analysis of Spatial Association by Use of Distance Statistics. Geographical Analysis 24(3):189–206

Goodwin S, Dykes J, Slingsby A, Turkay C (2016) Visualizing Multiple Variables Across Scale and Geography. Visualization and Computer Graphics, IEEE Transactions on 22(1):599 – 608

Guo D, Chen J, MacEachren AM, Liao K (2006) A visualization system for space-time and multivariate patterns (vis-stamp). IEEE transactions on visualization and computer graphics 12(6):1461–1474

Hadlak S, Tominski C, Schulz HJ, Schumann H (2010) Visualization of attributed hierarchical structures in a spatiotemporal context. International Journal of Geographical Information Science 24(10):1497–1513

Hering AS, Bell CL, Genton MG (2009) Modeling spatio-temporal wildfire ignition point patterns. Environmental and Ecological Statistics 16(2):225–250

Jacquez GM (1996) A k nearest neighbour test for space–time interaction. Statistics in medicine 15(18):1935–1949

Kapler T, Wright W (2005) Geotime information visualization. Information Visualization 4(2):136–146

Keim D, Andrienko G, Fekete JD, Görg C, Kohlhammer J, Melançon G (2008) Visual Analytics: Definition, Process, and Challenges. In: Kerren A, Stasko J, Fekete JD, North C (eds) Information Visualization, Lecture Notes in Computer Science, vol 4950, Springer Berlin Heidelberg, pp 154–175

Kisilevich S, Krstajic M, Keim D, Andrienko N, Andrienko G (2010) Event-based analysis of people's activities and behavior using flickr and panoramio geotagged photo collections. In: Information visualisation (IV), 2010 14th international conference, IEEE, pp 289–296

Knox EG, Bartlett MS (1964) The detection of space-time interactions. Applied Statistics pp 25–30

Kraak MJ, Ormeling F (2003) Cartography: visualisation of geospatial data. Essex: Pearson Education Limited

Lahouari K, Jean-Yves B, Paule-Annick D, Hlne M, Ccile SM (2014) Reprsenter les dynamiques des territoires : un tat des lieux, de nouveaux enjeux. URL `http://www.map.cnrs.fr/jyb/puca/`

Leipnik MR, Albert DP (2003) GIS in law enforcement: Implementation issues and case studies. CRC Press

Li S, Dragicevic S, Castro FA, Sester M, Winter S, Coltekin A, Pettit C, Jiang B, Haworth J, Stein A, et al. (2016) Geospatial big data handling theory and methods: A review and research challenges. ISPRS Journal of Photogrammetry and Remote Sensing 115:119–133

Lins L, Klosowski JT, Scheidegger C (2013) Nanocubes for real-time exploration of spatiotemporal datasets. Visualization and Computer Graphics, IEEE Transactions on 19(12):2456–2465

MacEachren AM, Jaiswal A, Robinson AC, Pezanowski S, Savelyev A, Mitra P, Zhang X, Blanford J (2011) Senseplace2: Geotwitter analytics support for situational awareness. In: Visual Analytics Science and Technology (VAST), 2011 IEEE Conference on, IEEE, pp 181–190

Maciejewski R, Rudolph S, Hafen R, Abusalah A, Yakout M, Ouzzani M, Cleveland WS, Grannis SJ, Ebert DS (2010) A visual analytics approach to understanding spatiotemporal hotspots. Visualization and Computer Graphics, IEEE Transactions on 16(2):205–220

Malik A, Maciejewski R, Collins TF, Ebert DS (2010) Visual analytics law enforcement toolkit. In: Technologies for Homeland Security (HST), 2010 IEEE International Conference on, IEEE, pp 222–228

Mantel N (1967) The detection of disease clustering and a generalized regression approach. Cancer research 27(2 Part 1):209–220

Miller HJ, Han J (2009) Geographic Data Mining and Knowledge Discovery. Chapman & Hall/CRC data mining and knowledge discovery series, CRC Press

Møller J, Ghorbani M (2010) Second-order analysis of structured inhomogeneous spatio-temporal point processes. Tech. rep., Department of Mathematical Sciences, Aalborg University

Moran PAP (1950) Notes on continuous stochastic phenomena. Biometrika pp 17–23

Openshaw S (1984) The modifiable areal unit problem. Concepts and techniques in modern geography

Ostfeld RS, Glass GE, Keesing F (2005) Spatial epidemiology: an emerging (or re-emerging) discipline. Trends in ecology & evolution 20(6):328–336

Robinson AC, Peuquet DJ, Pezanowski S, Hardisty FA, Swedberg B (2016) Design and evaluation of a geovisual analytics system for uncovering patterns in spatio-temporal event data. Cartography and Geographic Information Science pp 1–13

Roddick JF, Spiliopoulou M (1999) A bibliography of temporal, spatial and spatio-temporal data mining research. ACM SIGKDD Explorations Newsletter 1(1):34–38

Scherr M (2008) Multiple and coordinated views in information visualization. Trends in Information Visualization 38

Shanbhag P, Rheingans P, et al. (2005) Temporal visualization of planning polygons for efficient partitioning of geo-spatial data. In: Information Visualization, 2005. INFOVIS 2005. IEEE Symposium on, IEEE, pp 211–218

Shekhar S, Jiang Z, Ali RY, Eftelioglu E, Tang X, Gunturi V, Zhou X (2015) Spatiotemporal data mining: A computational perspective. ISPRS International Journal of Geo-Information 4(4):2306–2338

Silva R, Moura-Pires J, Santos MY (2012) Spatial Clustering in SOLAP Systems to Enhance Map Visualization. International Journal of Data Warehousing and Mining 8(2):23–43

Silva R, Pires JM, Santos MY, Datia N (2016) Enhancing exploratory analysis by summarizing spatiotemporal events across multiple levels of detail. In: Sarjakoski T, Santos MY, Sarjakoski TL (eds) Geospatial Data in a Changing World, Selected papers of the 19th AGILE Conference on Geographic Information Science, Lecture Notes in Geoinformation and Cartography, Springer, DOI 10.1007/978-3-319-33783-8_13, URL `https://link.springer.com/chapter/10.1007/978-3-319-33783-8\_13`

Silva RA, Pires JM, Santos MY (2015a) A granularity theory for modelling spatio-temporal phenomena at multiple levels of detail. International Journal of Business Intelligence and Data Mining 10(1):33

Silva RA, Pires JM, Santos MY, Leal R (2015b) Aggregating Spatio-temporal Phenomena at Multiple Levels of Detail. In: AGILE 2015, Springer Science \mathplus Business Media, pp 291–308

Sips M, Köthur P, Unger A, Hege HC, Dransch D (2012) A visual analytics approach to multiscale exploration of environmental time series. Visualization and Computer Graphics, IEEE Transactions on 18(12):2899–2907

Swedberg B, Peuquet D (2016) Perse visual analytics for calendar related spatiotemporal periodicity detection and analysis. GeoInformatica pp 1–21

Thakur S, Rhyne TM (2009) Data vases: 2d and 3d plots for visualizing multiple time series. In: International Symposium on Visual Computing, Springer, pp 929–938

Thom D, Bosch H, Koch S, Wörner M, Ertl T (2012) Spatiotemporal anomaly detection through visual analysis of geolocated twitter messages. In: Pacific visualization symposium (PacificVis), 2012 IEEE, IEEE, pp 41–48

Tominski C, Schulz HJ (2012) The Great Wall of Space-Time. In: Goesele M, Grosch T, Theisel H, Toennies K, Preim B (eds) Vision, Modeling and Visualization, The Eurographics Association, DOI 10.2312/PE/VMV/VMV12/199-206

Tominski C, Schulze-Wollgast P, Schumann H (2005) 3d information visualization for time dependent data on maps. In: Information Visualisation, 2005. Proceedings. Ninth International Conference on, IEEE, pp 175–181

Tversky B, Morrison JB, Betrancourt M (2002) Animation: can it facilitate? International journal of human-computer studies 57(4):247–262

Wang D, Ding W, Lo H, Morabito M, Chen P, Salazar J, Stepinski T (2013) Understanding the spatial distribution of crime based on its related variables using geospatial discriminative patterns. Computers, Environment and Urban Systems 39:93–106

Weaver C (2010) Cross-filtered views for multidimensional visual analysis. IEEE Transactions on Visualization and Computer Graphics 16(2):192–204

Yao JT, Vasilakos AV, Pedrycz W (2013) Granular computing: perspectives and challenges. IEEE Transactions on Cybernetics 43(6):1977–1989

Zhang L, Stoffel A, Behrisch M, Mittelstadt S, Schreck T, Pompl R, Weber S, Last H, Keim D (2012) Visual analytics for the big data eraA comparative review of state-of-the-art commercial systems. In: Visual Analytics Science and Technology (VAST), 2012 IEEE Conference on, IEEE, pp 173–182

Appendix A Abstracts Implemented

Measure	Description	Global	Spatial	Temporal
Bray-Curtis Similarity for Synthesis	Calculates the similarity based on the number of granular synthesis, between consecutive temporal grains		●	
Correlation Index For Atoms	Correlation between the number of atoms of consecutive temporal grains		●	
Correlation Index For Synthesis	Correlation between the number of granular synthesis of consecutive temporal grains		●	
Dice Similarity (Binary)	Dice index (event / no event) between consecutive temporal grains		●	
Jaccard Similarity (Binary)	Jaccard index (event / no event) between consecutive temporal grains		●	
Gower Similarity (Binary)	Similarity (event / no event) between consecutive temporal grains		●	
Moran's I	Calculates the spatial autocorrelation among nearby locations, given a domain specific variable		●	
Nearest Neighbor (NN)	Measures the level of clustering		●	●
Z-score Nearest Neighbor (z-NN)	Measures the z-score of the level of NN		●	●
Spatial Scope	Measures the spatial extent		●	
Spatial Consecutive Distance between Centers of Mass	Measures the distance between consecutive centers of mass		●	
Center's Mass Positioning	Measures the position of the centers of mass		●	●
Reduction Rate (%)	Measures the reduction of atoms used	●		
Average Atoms in spatiotemporal granules (%)	Measures the average of atoms indexed by spatiotemporal granules	●		

Measure	Description	Global	Spatial	Temporal
Collision Rate (%)	Percentage of spatiotemporal granules with events, where atom collisions exists	●	●	●
Occupation Rate (%)	Percentage of granules with events	●	●	●
Granular Mantel Bounded and Normalized	Measures the spatiotemporal interaction	●		
Frequency Rate (%)	Percentage of events happened in granules		●	●
Bray-Curtis Similarity for Atoms	Calculates the similarity based on the counts of atoms, between consecutive temporal grains		●	